The development of pyrene-conjugated oligonucleotide probes for RNA analysis

TAKAKO UEDA

2013

Kyoto Institute of Technology

Contents

Abbreviations

bcd	bicoid mRNA
cDNA	complementary oligodeoxyribonucleotide
cORN	complementary oligoribonucleotide
Cpy	2’-*O*-pyrenylmethylcytidine
eve	even-skipped mRNA
FRET	Förster resonance energy transfer
ftz	fushi-tarazu mRNA
gt	giant mRNA
hsa- mir	Homo sapiens microRNA
Kr	Krüppel mRNA
LNA	locked nucleic acid
miRNA	microRNA
nos	nanos mRNA
ODN	oligodeoxyribonucleotide
ORN	oligoribonucleotide
PNA	peptide nucleic acid
RISC	RNA-induced silencing complex
SARS	severe acute respiratory syndrome
snRNA	small nuclear RNA
Upy	2’-*O*-pyrenylmethyluridine

General Introduction

1. Background and objectives

RNA has been thought to be a molecule that reads nucleotide sequences from DNA and sends its information to the ribosome, when proteins are expressed from DNA having genetic information. However, many functional non-coding (nc) RNA was found in succession since miRNA was discovered in 1993 [1] and RNA came to be recognized as a molecule which had various functions in bio-regulation systems [2]. Now it is apparent that RNA is essential molecule acting on regulation of the genetic information and that it is deeply involved in development, differentiation, and the onset of diseases. 98 percent of the entire human genome is non-coding region and the blueprint for the protein was also revealed only about two per cent by extensive study of non-coding RNA [3, 4, 5]. It was estimated that each miRNA targets an average of 200 mRNA and more than one miRNA can act on a single mRNA target, suggesting that it is necessary to perform the study on the expression of the mRNA in more detail as well as miRNA [6, 7].The tool for the detection of RNA with swiftness, accuracy, and RNA-specificity will be very valuable to know the expression, localization, and movement of RNA. The elucidation of temporal and spatial function of RNA leads to the discovery of a network and bio-regulation system between molecules involved in biological phenomena which are not given from the gene sequence information. These discoveries will contribute to the development in the field of development, differentiation, regeneration, and medical diagnosis. In this thesis, I first described that target RNA expressed in *Drosophila melanogaster* embryo could be detected in the total RNA extracted from *Drosophila* embryos and in the fixed embryo using RNA-specific probe, OMUpy2. The expression levels of target RNA were also investigated with OMUpy2. In a multi-cellar tissue, *Drosophila* embryo, some genes are expressed time, positional specifically. For that, *Drosophila* embryo has caught my attention as an ideal system in which to evaluate the performance of the fluorescence probes, because the morphology and the emitting position make it possible to determine whether the fluorescence probe could detect target RNA. Second, I described that the average molecule numbers of RNA expressed

in a HeLa cell were estimated using OMUpy2. Third, the development of multicolored FRET RNA probes for the simultaneous observation of multiple target RNAs in a cell was described.

2. Fluorescence *in situ* hybridization

Fluorescence *in situ* hybridizationis (FISH) a method to detect the target gene hybridized by a probe labeled with a fluorescent substance or an enzyme under a fluorescent microscope. *in situ* hybridization (ISH) is a technique that was developed by Pardue and Gall [8] and John et al [9] in 1969, however their technique contained several problems because of utilizing probes labeled with radioisotopes. First, the isotope decays over time so the specific activity of a probe is not constant and unstable. Second, the resolution is limited for the dispersion accompanied with radioactive decay although sensitivity of radiography is generally high. Third, long exposure times are required to detect signals. Fourth, radioisotope-labeled probe is relatively costly and hazardous material [10]. Therefore histochemical detection method became available using alkaline-phosphatase-coupled antibodies that detect Digoxigenin (DIG) labeled probes [11-13]. This method demands considerably less skill compared with ISH using radioisotope-labeled probe. These developments have further advanced and the first application of fluorescence *in situ* hybridization was reported in 1980. The RNA directly labeled with fluorescent molecules to the 3’ end was used as a probe [14]. FISH has developed as an alternative to previous methods for visualization of RNA in terms of resolution, speed, safety, simultaneous detection of multiple RNA targets, quantitative analysis, and imaging in living cells..

3. Oligonucleotide probes

ISH detection of mRNA has been commonly performed using RNA probes transcribed from cDNA copy of the mRNA target [15, 16]. Therefore probes are several hundreds or thousands of nucleotides long and contain repeat sequences that cause high background fluorescence by nonspecifically binding [17]. ISH for the detection of RNA in fixed specimen with long probes relies on the steps to open the RNA target sequence

and allow specifically binding of the long probes by annealing. The available sequences in RNA target are also limited because certain sequences are unfound in cDNA library, or certain cDNA is difficult to gain. Furthermore, the amount of long probes cannot be determined quantitatively because labeling molecules such as fluorescent molecules and DIG are incorporated into RNA probes every 10-15nt at random. RNA probes produced from cDNA are also easily degraded by RNase. Though long probes have been introduced into living cells using microinjection to visualize the localization of a specific RNA [18-20], this approach cannot be applied to the detection of endogenous RNA in living cells.

Oligonucleotide probes using modified nucleic acid bases have been resolved many of these problems. Commonly chemical synthesized FISH probes employ 15–30 nucleotides long with a DNA, RNA, or modified nucleic acid backbone. Fluorescence is directly observed using a fluorophore attached to the 5'- or 3'-terminus, or internally labeled probes. The sequences of oligonucleotide probes are able to be designed *in silico*, and easily synthesized compared with RNA probes made from cDNA. It is also confirmed that oligonucleotide probes hybridize specifically to the complementary RNA by the melting curve analysis. Methods based on the hybridization with a fluorescent labeled oligonucleotides probe have been able to extend to the application in living cells since linear probes enable to access to the target site of long RNA target without annealing to open the target site for binding.

In 1989, fluorescein labeled oligonucleotide probes and rhodamine labeld oligonucleotide probes hybridized to 16S ribosomal RNA (rRNA) in the fixed cells and visualized its existence under a fluorescence microscope [21]. The Studies using rhodamine labeld oligonucleotide probes targeting for ribosomal RNA (rRNA) were also performed as a means of analysis [22, 23]. These studies with fluorescent labeled oligonucleotide probes led to studies on poly (A) RNA in living cells.

In 1995, first detection of RNA in living cells using fluorescent (Texas Red) labeled oligodeoxynucleotides was reported by Politz *et al.* [24]. In this report, it was shown that phosphorothioate and fluorescent labeled phosphodiester oligo dT entered cells rapidly and hybridized to poly (A) RNA within 30 min [24]. In 1998, intranuclear

diffusion of poly (A) RNA was observed with fluoresein labeled oligodeoxynucleotide in living cells [25]. The main problem accompanied with the use of these probes for visualization of the distributed RNA is the low signal to noise ratio. That occurs by the reason why the emitting from unhybridized probes is strong and the signal from target RNA is small. This problem can be resolved by the probe which emits only when it binds to target RNA.

4. FRET probes

FRET (Förster Resonance Energy Transfer) is one of the fluorescence-related phenomena. A photon from an energetically excited fluorophore, the donor, raises the energy state of an electron in another molecule, the acceptor, to higher vibrational levels of the excited singlet state. As a result, the energy level of the donor fluorophore returns to the ground state, without emitting fluorescence. This mechanism is dependent on the dipole orientations of molecules and is limited by the distance between the donor and the acceptor molecules. Typical effective distances between the donor and acceptor molecules are in the 10 to 100 Å range. This range is the distance between three to thirty nucleotides located in the double helix of a DNA molecule. Another requirement is that the fluorescence emission spectrum of the donor must overlap the absorption spectrum of the acceptor. The acceptor can be another fluorophore or a non-fluorescent molecule. If the acceptor is a fluorophore, the transferred energy can be emitted as fluorescence [26]. In 1988, it was reported that FRET was caused to rhodamine (acceptor) from fluorescein (donor) covalently attached to the 5’ ends of oligonucleotides. These results showed the hybridization of nucleic acid could be detected by FRET [27]. Various studies on structural analysis [28-33] and oligonucleotide hybridization [34-37] by FRET have been reported. These FRET techniques with further development proved useful for detection and quantify of nucleic acid hybridization in living cells. In 2000, Tsujii *et al.* observed, for the first time, human c-*fos* mRNA expressed at more than 10^4 molecules in a living transfected Cos7 cell by FRET probes (Bodipy493/503 and Cy5 was used as a donor and an acceptor) under a fluorescence microscope [38]. Then they developed a method not affected by the cell autofluorescence to detect smaller number

of RNA with a time resolved fluorescence microscopy and visualized the presence of c-*fos* mRNA in HeLa cells using FRET probes [39].

5. 2'-*O*-methyl RNA, LNA, PNA

In order to overcome the problems of the degradation of oligo nucleotide probes by an enzyme and the sufficient affinity with the target RNA in the cell, nucleic acid probes having a non-natural backbone such as, 2'-*O*-methyl RNA, locked nucleic acid (LNA), and peptide nucleic acid (PNA) have been developed [40-45]. Because the thermal stability of the hybrids of the artificial nucleic acid probes and RNA is higher than that of the base paring between the DNA-RNA, it is possible to suppress the false signal by nonspecific binding.

2'-*O*-methyl RNA probes have been reported to form very stable hybrids with target RNA in terms of high melting temperature. Further, because of the low cost, 2'-*O*-methyl RNA probes is most commonly used to detect RNA or to inhibit the target gene expression. Majlessi *et al*. showed that 2'-*O*-methyl RNA probes exhibit higher affinity for target RNA than the corresponding 2'-deoxyoligoribonucleotide (ODN) probes resulting in higher melting temperatures [45]. The affinity of 2'-*O*-methyl RNA probes and RNA was the highest in 2'-*O*-methyl RNA probes and DNA, ODN probes and RNA, and ODN probes and DNA [45]. In addition to the enhancement of Tm value, they revealed that 2'-*O*-methyl RNA probes hybridized 2- to 4-fold faster to RNA than ODN probes [45]. Therefore 2'-*O*-methyl RNA probes greatly have advantages over ODN probes for detecting RNA. 2'-*O*-methyl RNA probes also have high resistance to enzymatic [46-49]. In 2001, Molenaar *et al.* confirmed that cells microinjected with the 2'-*O*-methyl RNA probes could be monitored for several days [46]. The half-life of DNA probes injected in the living cells was shown to be about 15 min [47]. Czauderna *et al.* also reported that the effect of gene expression inhibition in RNAi experiments using dsRNA containing 2'-*O*-methyl RNA remained for five days [48].

Locked nucleic acid (LNA) LNA is a nucleic acid analogue containing a 2'-O, 4'-C methylene bridge [50]. This methylene moiety causes a change in the conformation of nucleic acid helices and increases thermal stability to form the A-form

duplexes. LNA was independently synthesized by the group of Takeshi Imanishi in 1997 [50], and by the group of Jesper Wengel in 1998 [51]. LNA oligonucleotides display unprecedented hybridization affinity toward complementary RNA and complementary DNA [52-55]. A new method for highly efficient detection of microRNAs by northern blot analysis using LNA (Locked Nucleic Acid)-modified oligonucleotides was shown by Valoczi *et al.* [56]. They designed DNA probes containing LNA for microRNAs in animals and plants. Using the DNA probes substituted by LNA at every three position in northern blot analysis employing standard end-labeling techniques and hybridization conditions, the sensitivity of detection signals increased at least 10-fold compared to conventional DNA probes [56]. In fixed cells, LNA probes detected target RNA with far better efficiency than conventional DNA probes [57]. LNA probes have also been used to detect 21-22-nt microRNAs by whole mount *in situ* hybridization [58, 59]. Darnell *et al*. employed LNA modified DNA probes (12-24-nt), containing an LNA nucleotide at every three position and labeld at the 5' end with DIG, to visualize the localization of mRNA in fixed chicken embyos [60]. They also showed the detection of alternatively spliced exon using LNA probes [60]. The problems are high cost and unavailability unlike 2'-*O*-methyl RNA to be able to freely design and synthesize.

The main bone of PNA consists from N- (2-aminoethyl) glycine linked by an amide bond instead of sugar in a nucleic acid. Purine ring and pyrimidine ring corresponding to the nucleobase are bound to the main chain through a methylene group and a carbonyl group. Since the charge of the phosphate site such as DNA or RNA is not present in PNA, the duplex of PNA/DNA and PNA/RNA are formed strongly than DNA/DNA, RNA/DNA, and RNA/RNA by a decrease in electrostatic repulsion [61]. However, PNA is so rigid molecules that it is difficult to access to highly folded RNA structures and therefore PNA have not been used as a hybridization probe in living cells [62].

6. Molecular beacons

Molecular beacons (MB) were first developed by Tyagi *et al*. in 1996 as a tool for real-time PCR assays [63, 64]. Molecular beacons are ODNs that form a stem-loop

hairpin structure and are dual-labeled with a reporter fluorophore at one end and a quencher at the other. In the absence of a complementary target, the molecular beacon is in a stem-loop configuration in which the fluorescence is quenched. Following hybridization to a complementary target, the hairpin structure is changed to an open configuration separating the fluorophore and quencher and restoring fluorescence [65]. The obstacle in monitoring the localization or movements of RNA transcribing in living cells with the typical fluorescent probes is the emission of fluorescent labeled probes before hybridizing to target RNA. This makes it difficult to trace the origin of movements, and fate of the specific RNA. Molecular beacon has improved this problem.

In 1998, the first application of molecular beacons to the probe for mRNA detection was reported [66, 67] and many studies to track the movement of RNA using molecular beacons were performed [68-71]. Though the backbone of early molecular beacons was DNA, molecular beacons came to be synthesized with 2'-*O*-methyl RNA backbone in order to improve the lack of resistance enzyme and low reproducibility [68, 72, 73]. The thermodynamic and kinetic properties of the hybridization between 2'-*O*-methyl RNA molecular beacons and RNA were improved more stable compared to DNA molecular beacons. And the problem of false-positive signals caused by DNA molecular beacons degraded by nuclease in living cells is resolved. However, 2'-*O*-methyl molecular beacons is lower performance compared with linear 2'-*O*-methyl RNA probe and in particular the signal intensity observed with 2'-*O*-methyl molecular beacons was 2-3-fold lower compared with linear 2'-*O*-methyl RNA probe [48, 68]. 2'-*O*-methyl molecular beacons also have time-lag until emitting the maximum signal because they are in a closed and quenched form. Therefore initial signal intensity is very low. In the report by Molenaar *et al*., from 5-10 min after microinjection, the signal intensity increased steadily throughout the nucleus and similar localization patterns were observed as obtained with linear 2'-*O*-methyl RNA probes [46].

To improve signal-to-noise ratio, molecular beacons using FRET have been developed. If the optimal emission wavelength is only a few nanometers longer than the

optimal excitation wavelength (Stokes shift) a portion of the excitation light can reach the detector by scattering and reflection, thus limiting detection sensitivity. On the other hand the large Stokes shifts of wavelength-shifting molecular beacons allow more effective filtering of the excitation light, thereby enhancing the sensitivity of target detection. Large Stokes shifts are particularly significant in the detection of the hybrids of probes and target RNA in living cells, where autofluorescence of cellular components introduces a background signal. This approach was first tried with wavelength shifting molecular beacons in multiplex PCR assays [74]. Dual FRET molecular beacons were also designed to detect high sensitively specific endogenous mRNA in living cells. [71, 75] Dual FRET molecular beacons consisted of two molecular beacons. One beacon was labeled with a donor fluorophore and second beacon was labeled with an acceptor fluorophore. These two molecular beacons were designed to hybridize to adjacent regions on a target mRNA to occur an energy transfer between two molecular beacons when both beacons hybridized to target mRNA. The fluorescence emission of acceptor fluorophore cannot be observed unless donor fluorophore is excited, which enables to distinguish readily the positive signals and the false positive signals caused by probe degradation and nonspecific probe opening [76]. In 2004, Santangelo *et al*. showed the detection of only a few hundred copies of an endogenous mRNA in a single living cell would be feasible with dual FRET molecular beacons [71]. Using dual FRET molecular beacons, the localization of *oskar* mRNA in *Drosophila* oocytes could be confirmed *in vivo* [73]. Further by Mhlanga *et al*., a more refined model of *oskar* mRNA transport in the *Drosophila* oocyte were revealed using molecular beacons designed by Bratu *et al*. [73, 77]. However, molecular beacons have not yet been able to detect other mRNAs in *Drosophila* embryos.

7. The developments of *Drosophila* embryo

The early development of the fruit fly, *Drosophila* melanogaster, is better understood than that of any other animal. Astonishing discoveries in developmental biology over the past 30 years have revealed that many of the genes that control the development of *Drosophila* are similar to those controlling development in vertebrates,

and many other animals.

The *Drosophila* embryo is a multiple-cellar tissue and in which the genes involved in early development show unique expression patterns. The *Drosophila* egg is rather oblong and the anterior end is easily recognizable by the micropyle, a nipple-shaped structure in the tough external coat surrounding the egg. Sperm enter the anterior end of the egg through the micropyle. After fertilization and fusion of the sperm and egg nuclei, the zygote nucleus undergoes a series of rapid mitotic divisions, one about every 9 minutes, but, unlike in most other animal embryos, there is initially no cleavage of the cytoplasm and no formation of cell membranes to separate the nuclei. The result after 12 nuclear divisions is a syncytium in which around 6,000 nuclei are present in a common cytoplasm. Early development of a *Drosophila* embryo is extremely rapid. The first 13 nuclear divisions are completed in just over 3 hours and occur in the absence of cytokinesis, producing an embryo of about 6,000 nuclei in a common cytoplasm. During these syncytial divisions, the body axes and segments are established. The dividing nuclei progress through an orchestrated series of migrations to situate in a well-organized monolayer of nuclei at the actin-rich cortex. These events occur on a time-scale of minutes, many of the nuclear cycles are less than 10 minutes. In spite of the speed and crowding of the nuclei, the fidelity of these events is high [78-80].

The *Drosophila* embryo is patterned with a distinct polarity along its anterior-posterior axis. The groundwork for this pattern is organized by the maternal mRNA and protein which is deposited in the egg during oogenesis [81]. The patterning along the anterior-posterior axis which leads to the segmentation of a body depends on the Bicoid and Nanos gradients [82, 83] (Figure 1.). Hunchback is distributed throughout the embryo as a maternal mRNA. However, Bicoid activates Hunchback transcription anteriorly, and Nanos which is a mRNA-binding protein blocks the translation of Hunchback transcripts posteriorly. Therefore the concentration gradient of Hunchback is formed from the anterior toward posterior [84]. The gradient of Hunchback dictates where the gap genes, such as Krüppel, Knirps, and Giant, are expressed by providing a series of concentration thresholds that regulate each gene

independently. Thus Hunchback triggers several distinct responses as a function of its graded distribution [84-88]. Based on the anterior-posterior axis which is defined by the first gradient of Bicoid and Nanos, a body plan is formed more precisely by segmentation genes. Segmentation genes are classified into three groups, gap genes, pair-rule gene, and segmental polarity genes. First, the concentration gradient of maternal effect genes act on gap genes and their products roughly divide an embryo into each part which are based on the next cascade. Then, pair-rule genes are expressed by the effects of gap genes and form the segments. Further, segmental polarity genes induced by a prepattern of pair-rule gene products are expressed and define domains in more detail [89-92].

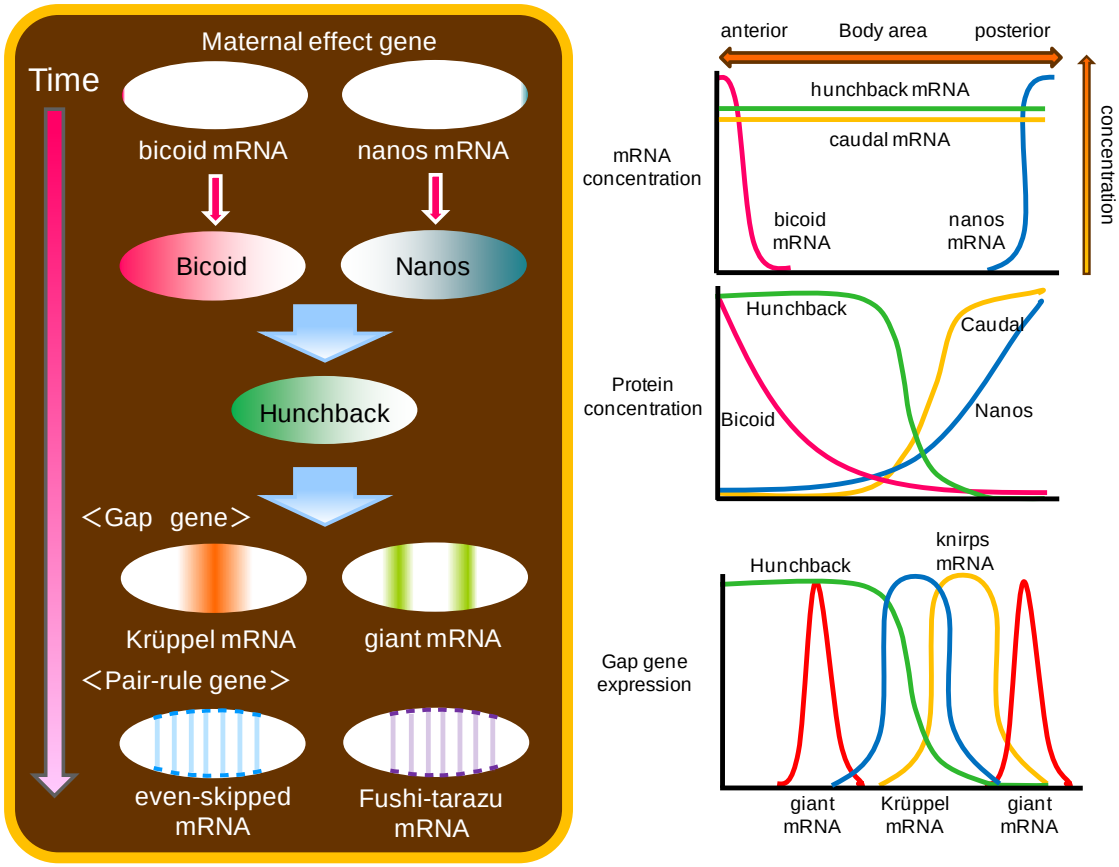

Figure 1. A model of anterior-posterior pattern generation by *Drosophila* maternal effect genes

The bicoid, nanos, hunchback, and caudal mRNAs are placed in the oocyte by the ovarian nurse cells. The Bicoid protein gradient extends to from anterior to posterior, and Nanos protein gradient extends from posterior to anterior. Nanos inhibits the translation of hunchback mRNA, while Bicoid prevents the translation of the caudal mRNA. This inhibition results in opposing Caudal and Hunchbask gradients. The gap genes expression patterns are determined by the gradients of protein products of Bicoid, Caudal, and Hunchback. Gap genes establish the segmented body plan of the embryo along the longitudinal axis. The RNA of each of the gap genes has very distinct distribution that defines abutting or slightly overlapping regions of expression. Their protein products control the more detail expression patterns of the pair-rule genes [92].

References

1. Lee, R.C., Feinbaum, R.L., Ambros, V. (1993) The C. elegans heterochronic gene lin-4 encodes small RNAs with antisense complementarity to lin-14. *Cell*, 75, 843-854.
2. Eddy, S.R. (2001) Non-coding RNA genes and the modern RNA world. *Nature Reviews Genetics*, 2, 919-929.
3. Wilusz, .J.E., Sunwoo, H., Spector, D.L. (2009) Long noncoding RNAs: functional surprises from the RNA world. *Genes Dev*., 23, 1494-1504.
4. Mattick, J.S., Makunin, I.V. (2006) Non-coding RNA. *Hum. Mol. Genet*. 15, 1, R17-29.
5. Mattick, J.S. (2005) The functional genomics of noncoding RNA. *Science*, 309, 5740, 1527-1528.
6. Zhang, W., Edwards, A., Fan, W., Flemington, E.K., Zhang, K. (2012) miRNA-mRNA correlation-network modules in human prostate cancer and the differences between primary and metastatic tumor subtypes. *PLoS One*., 7, e40130.
7. Muniategui, A., Pey, J., Planes, F.J., Rubio, A. (2013) Joint analysis of miRNA and mRNA expression data. *Brief. Bioinform*., 14, 263-278.
8. Pardue, M.L., Gall, J.G. (1969) Molecular hybridization of radioactive DNA to the DNA of cytological preparations. *Proc. Natl. Acad. Sci. U.S.A.*, 64, 600-604.
9. John, H.A., Birnstiel, M.L., Jones, K.W. (1969) RNA-DNA hybrids at the cytological level. *Nature*, 223, 582-587.
10. Levsky, J.M., Singer, R.H. (2003) Fluorescence *in situ* hybridization: past, present and future. *J. Cell Sci.*, 116, 2833-2838.
11. Edgar, B.A., Odell, G.M., Schubiger, G. (1987) Cytoarchitecture and the patterning of fushi tarazu expression in the *Drosophila* blastoderm. *Genes Dev*., 1, 1226-1237.
12. Tautz, D., Pfeifle, C. (1989) A non-radioactive *in situ* hybridization method for the localization of specific RNAs in *Drosophila* embryos reveals translational control of the segmentation gene hunchback. *Chromosoma*, 98, 81-85.
13. Holtke, H.J., Kessler, C. (1990) Non-radioactive labeling of RNA transcripts *in vitro* with the hapten digoxigenin (DIG); hybridization and ELISA based detection. *Nucleic Acids Res.*, 18, 19, 5843-5851.
14. Bauman, J.G., Wiegant, J., Borst, P., van Duijn, P. (1980) A newmethod for fluorescence microscopical localization of specific DNA sequences by *in situ* hybridization of fluorochromelabelled RNA. *Exp. Cell Res.*, 128, 485-490.
15. Melton, D.A., Krieg, P.A., Rebagliati, M.R., Maniatis, T., Zinn, K., Green, M.R. (1984) Effcient *in vitro* synthesis of biologicafly active RNA and RNA hybridization probes from plasmids containing a bacteriophage SP6 promoter. *Nucleic Acids Res.*, 12, 18, 7035-7056.

16. Landegent, J.E., Jansen, in de Wal N., Dirks, R.W., Baao, F., van der Ploeg, M. (1987) Use of whole cosmid cloned genomic sequences for chromosomal localization by non-radioactive *in situ* hybridization. *Hum Genet.*, 77, 366-370.
17. Kobayashi, S., Saito, H., Okada, M. (1994) A simplified and efficient method for *in situ* hybridization to whole *Drosophila* embryos, using electrophoresis for removing non- hybridized probes. *Develop. Growth & Differ.*, 36, 6, 629-632.
18. Yisraeli, J.K., Melton, D.A. (1988) The material mRNA Vg1 is correctly localized following injection into Xenopus oocytes. *Nature*, 336, 6199, 592-595.
19. Wang, J., Cao, L.G, Wang, Y.L, Pederson, T. (1991) Localization of pre-messenger RNA at discrete nuclear sites. *Proc. Natl. Acad. Sci. U.S.A.*, 88, 16, 7391-7395.
20. Ainger, K., Avossa, D., Morgan, F., Hill, S.J., Barry, C., Barbarese, E., Carson, J.H. (1993) Transport and localization of exogenous myelin basic protein mRNA microinjected into oligodendrocytes. *J. Cell Biol.*, 123, 2, 431-441.
21. DeLong, E.F., Wickham, G.S., Pace, N.R. (1989) Phylogenetic stains: ribosomal RNA-based probes for the identification of single cells. *Science*, 243, 4896, 1360-1363.
22. Amann, R.I., Binder, B.J., Olson, R.J., Chisholm, S.W., Devereux, R., Stahl, D.A. (1990) Combination of 16S rRNA-Targeted Oligonucleotide Probes with Flow Cytometry for Analyzing Mixed Microbial Populations. *Appl Environ Microbiol.*, 56, 6, 1919-1925.
23. Amann, R.I., Krumholz, L., Stahl, D.A.(1990) Fluorescent-Oligonucleotide Probing of Whole Cells for Determinative, Phylogenetic, and Environmental Studies in Microbiology. J. *Bacteriol.*, 172, 2, 762-770.
24. Politz, J.C., Taneja, K.L., Singer, R.H. (1995) Characterization of hybridization between synthetic oligodeoxynucleotides and RNA in living cells. *Nucleic Acids Res.*, 23, 24, 4946-4953.
25. Politz, J.C., Browne, E.S., Wolf, D.E., Pederson, T. (1998) Intranuclear diffusion and hybridization state of oligonucleotides measured by fluorescence correlation spectroscopy in living cells. *Proc. Natl. Acad. Sci. U.S.A.*, 95, 11, 6043-6048.
26. Marras, S.A. (2006) Selection of fluorophore and quencher pairs for fluorescent nucleic acid hybridization probes. *Methods Mol Biol.*, 335, 3-16.
27. Cardullo, R.A., Agrawal, S., Flores, C., Zamecnik, P.C., Wolf, D.E. (1988) Detection of nucleic acid hybridization by nonradiative fluorescence resonance energy transfer. *Proc. Natl. Acad. Sci. U.S.A.*, 85, 8790-8794.
28. Tuschl, T., Gohlke, C., Jovin, T.M., Westhof, E., Eckstein, F. (1994) A three-dimensional model for the hammerhead ribozyme based on fluorescence measurements. *Science*, 266, 785–789.
29. Mergny, J.L., Boutorine, A.S., Garestier, T., Belloc, F., Rougée, M., Bulychev, N.V., Koshkin, A.A., Bourson, J., Lebedev, A.V., Valeur, B., et al. (1994)

Fluorescence energy transfer as a probe for nucleic acid structures and s equences. *Nucleic Acids Res*., 22, 6, 920-928.

30. Clegg, R.M., Murchie, A.I., Zechel, A., Lilley, D.M. (1993) Observing the helical geometry of double-stranded DNA in solution by fluorescence resonance energy transfer. *Proc. Natl. Acad. Sci. U.S.A*., 90, 7, 2994-2998.
31. Jares-Erijman, E.A., Jovin, T.M. (1996) Determination of DNA helical handedness by fluorescence resonance energy transfer. *J. Mol. Biol.* 257, 597–617.
32. Cooper, J.P., Hagerman, P.J. (1990) Analysis of fluorescence energy transfer in duplex and branched DNA molecules. *Biochemistry*. 29, 39, 9261-9268.
33. Gohlke, C., Murchie, A.I., Lilley, D.M., Clegg, R.M. (1994) Kinking of DNA and RNA helices by bulged nucleotides observed by fluorescence resonance energy transfer. *Proc. Natl. Acad. Sci.U.S.A.*, 91, 24, 11660–11664.
34. Ghosh, S.S., Eis, P.S., Blumeyer, K., Fearon, K., Millar, D.P. (1994) Real time kinetics of restriction endonuclease cleavage monitored by fluorescence resonance energy transfer. *Nucleic Acids Res*., 22, 15, 3155–3159.
35. Parkhurst, K M , Parkhurst, L.J. (1995) Kinetic studies by fluorescence resonance energy transfer employing a double-labeled oligonucleotide: hybridization to the oligonucleotide complement and to single-stranded DNA. *Biochemistry*. 34, 1, 285-92.
36. Bjornson, K.P., Amaratunga, M., Moore, K.J., Lohman, T.M. (1994) Single-turnover kinetics of helicase-catalyzed DNA unwinding monitored continuously by fluorescence energy transfer. *Biochemistry*. 33, 47, 14306-14316.
37. Yang, M., Ghosh, S.S., Millar, D.P. (1994) Direct measurement of thermodynamic and kinetic parameters of DNA triple helix formation by fluorescence spectroscopy. *Biochemistry*. 33, 51, 15329-15337.
38. Tsuji, A., Koshimoto, H., Sato, Y., Hirano, M., Sei-Iida, Y., Kondo, S., Ishibashi, K. (2000) Direct Observation of Specific Messenger RNA in a Single Living Cell under a Fluorescence Microscope. *Biophys J.* 78, 6, 3260-3274.
39. Tsuji, A., Sato, Y., Hirano, M., Suga, T., Koshimoto, H., Taguchi, T., Ohsuka, S. (2001) Development of a time-resolved fluorometric method for observing hybridization in living cells using fluorescence resonance energy transfer. *Biophys J*. 81, 1, 501-515.
40. Egholm, M., Buchardt, O., Christensen, L., Behrens, C., Freier, S.M., Driver, D.A., Berg, R.H., Kim, S.K., Norden, B., Nielsen, P.E. (1993) PNA hybridizes to complementary oligonucleotides obeying the Watson-Crick hydrogen-bonding rules. *Nature*, 365, 6446, 66-68.
41. Egholm, M., Buchardt, O., Nielsen, P.E., Berg, R.H. (1992) Peptide nucleic acids (PNA). Oligonucleotide analogs with an achiral peptide backbone. *J. Am. Chem. Soc*., 114, 5, 1895-1897.
42. Braasch, D.A., Corey, D.R. (2001) Locked nucleic acid (LNA): fine-tuning the recognition of DNA and RNA. *Chem Biol*., 8, 1, 1-7.

43. Boulmé, F., Freund, F., Moreau, S., Nielsen, P.E., Gryaznov, S., Toulmé, J.J., Litvak, S. (1998) Modified (PNA, 2'-*O*-methyl and phosphoramidate) anti-TAR antisense oligonucleotides as strong and specific inhibitors of in vitro HIV-1 reverse transcription. *Nucleic Acids Res*., 26, 23, 5492-5500.
44. Stein, D., Foster, E., Huang, S.B., Weller, D., Summerton, J. (1997) A Specificity Comparison of Four Antisense Types Morpholino, 2'-*O*-Methyl RNA, DNA, and Phosphorothioate DNA. *Antisense Nucleic Acid Drug Dev.*, 7, 3, 151-157.
45. Majlessi, M., Nelson, N.C., Becker, M.M. (1998) Advantages of 2'-*O*-methyl oligoribonucleotide probes for detecting RNA targets. *Nucleic Acids Res*., 26, 9, 2224-2229.
46. Molenaar, C., Marras, S.A., Slats, J.C., Truffert, J.C., Lemaître, M., Raap, A.K., Dirks, R.W., Tanke, H.J. (2001) Linear 2'*O*-Methyl RNA probes for the visualization of RNA in living cells. *Nucleic Acids Res*., 29, 17, E89-9.
47. Sixou, S., Szoka, F.C. Jr, Green, G.A., Giusti, B., Zon, G., Chin, D.J. (1994) Intracellular oligonucleotide hybridization detected by fluorescence resonance energy transfer (FRET). *Nucleic Acids Res*., 22, 4, 662–668.
48. Czauderna, F., Fechtner, M., Dames, S., Aygün, H., Klippel, A., Pronk, G.J., Giese, K., Kaufmann, J. (2003) Structural variations and stabilising modifications of synthetic siRNAs in mammalian cells. *Nucleic Acids Res*., 31, 11, 2705-2716.
49. Kubota, T., Ikeda, S., Yanagisawa, H., Yuki, M., Okamoto, A. (2009) Hybridization-sensitive fluorescent probe for long-term monitoring of intracellular RNA. Bioconjug Chem., 20, 6, 1256-1261.
50. Obika, S., Nanbu, D., Haria, Y., Morioa, K., In, Y., Ishida, T., Imanishia, T. (1997) Synthesis of 2'-*O*, 4'-C-methyleneuridine and -cytidine. Novel bicyclic nucleosides having a fixed C3, -endo sugar puckering. *Tetrahedron Lett*., 38, 50, 8735–8738.
51. Koshkin, A.A, Singh, S.K., Nielsen, P., Rajwanshi, V.K., Kumar, R., Meldgaard, M., Olsen, C. E., Wengel, J. (1998) LNA (Locked Nucleic Acids): Synthesis of the adenine, cytosine, guanine, 5-methylcytosine, thymine and uracil bicyclonucleoside monomers, oligomerisation, and unprecedented nucleic acid recognition. *Tetrahedron*, 54, 14, 3607–3630.
52. Singh, S.K., Wengel, J. (1998) Universality of LNA-mediated high-affinity nucleic acid recognition. *Chem. Commun*., 12, 1247-1248
53. Vester, B., Wengel, J. (2004) LNA (Locked Nucleic Acid): High-Affinity Targeting of Complementary RNA and DNA. *Biochemistry*. 43, 42, 13233-13241.
54. Sørensen, M.D., Petersen, M., Wengel, J. (2003) Functionalized LNA (locked nucleic acid): high-affinity hybridization of oligonucleotides containing N-acylated and N-alkylated 2'-amino-LNA monomers. *Chem Commun*., 17, 2130-2131.

55. Braasch, D.A., Corey, D.R. (2001) Locked nucleic acid (LNA): fine-tuning the recognition of DNA and RNA. *Chem. Biol*., 8, 1, 1-7.
56. Válóczi, A., Hornyik, C., Varga, N., Burgyán, J., Kauppinen, S., Havelda, Z. (2004) Sensitive and specific detection of microRNAs by northern blot analysis using LNA-modified oligonucleotide probes. *Nucleic Acids Res*., 32, 22, e175.
57. Thomsen, R., Nielsen, P.S., Jensen, T.H. (2005) Dramatically improved RNA *in situ* hybridization signals using LNA-modified probes. *RNA*, 11, 11, 1745-1748.
58. Wienholds, E., Kloosterman, W.P., Miska, E., Alvarez-Saavedra, E., Berezikov, E., de Bruijn, E., Horvitz, H.R., Kauppinen, S., Plasterk, R.H. (2005) MicroRNA expression in zebrafish embryonic development. *Science*, 309, 5732, 310-311.
59. Kloosterman, W.P., Wienholds, E., de Bruijn, E., Kauppinen, S., Plasterk, R.H. (2006) *In situ* detection of miRNAs in animal embryos using LNA-modified oligonucleotide probes. *Nat. Methods*, 3, 1, 27-29.
60. Darnell, D.K., Stanislaw, S., Kaur, S., Antin, P.B. (2010) Whole mount *in situ* hybridization detection of mRNAs using short LNA containing DNA oligonucleotide probes. *RNA*, 16, 3, 632-637.
61. Jensen, K.K., Orum, H., Nielsen, P.E., Nordén, B. (1997) Kinetics for hybridization of peptide nucleic acids (PNA) with DNA and RNA studied with the BIAcore technique. *Biochemistry*, 36, 16, 5072-5077.
62. Menchise, V., De Simone, G., Tedeschi, T., Corradini, R., Sforza, S., Marchelli, R., Capasso, D., Saviano, M., Pedone, C. (2003) Insights into peptide nucleic acid (PNA) structural features: the crystal structure of a D-lysine-based chiral PNA-DNA duplex. *Proc. Natl. Acad. Sci. U.S.A.*, 100, 21, 12021-12026.
63. Tyagi, S., Kramer, F.R. (1996) Molecular beacons: probes that fluoresce upon hybridization. *Nat Biotechnol*., 14, 3, 303-308.
64. Tyagi, S., Bratu, D.P., Kramer, F.R. (1998) Multicolor molecular beacons for allele discrimination. *Nat Biotechnol*., 16, 1, 49-53.
65. Dirks, R.W., Tanke, H.J. (2006) Advances in fluorescent tracking of nucleic acids in living cells. *Biotechniques*, 40, 4, 489-496.
66. Matsuo T. (1998) *In situ* visualization of messenger RNA for basic fibroblast growth factor in living cells. *Biochim Biophys Acta*., 1379, 2, 178-184.
67. Sokol, D.L., Zhang, X., Lu, P., Gewirtz, A.M. (1998) Real time detection of DNA. RNA hybridization in living cells. *Proc. Natl. Acad. Sci. U.S.A.*, 95, 20, 11538-11543.
68. Tyagi, S., Alsmadi, O. (2004) Imaging native beta-actin mRNA in motile fibroblasts. *Biophys J.*, 87, 6, 4153-4162.
69. Nitin, N., Santangelo, P.J., Kim, G., Nie, S., Bao, G. (2004) Peptide-linked molecular beacons for efficient delivery and rapid mRNA detection in living cells. *Nucleic Acids Res.*, 14, 32, 6, e58.
70. Cui, Z.Q., Zhang, Z.P., Zhang, X.E., Wen, J.K., Zhou, Y.F., Xie, W.H. (2005) Visualizing the dynamic behavior of poliovirus plus-strand RNA in living host

cells. *Nucleic Acids Res*., 33, 10, 3245-3252.

71. Santangelo, P.J., Nix, B., Tsourkas, A., Bao, G. (2004) Dual FRET molecular beacons for mRNA detection in living cells. *Nucleic Acids Res.*, 32, 6, e57.
72. Tsourkas, A., Behlke, M.A., Bao, G. (2003) Hybridization of 2'-*O*-methyl and 2'-deoxy molecular beacons to RNA and DNA targets. *Nucleic Acids Res.*, 31, 6, 5168-5174.
73. Bratu, D.P., Cha, B.J., Mhlanga, M.M., Kramer, F.R., Tyagi, S. (2003) Visualizing the distribution and transport of mRNAs in living cells. *Proc. Natl. Acad. Sci. U.S.A.*, 100, 23, 13308-13313.
74. Tyagi, S., Marras, S.A., Kramer, F.R. (2000) Wavelength-shifting molecular beacons. Nat. Biotechnol., 18, 11, 1191-1196.
75. Tsourkas, A., Behlke, M.A., Xu, Y., Bao, G. (2003) Spectroscopic features of dual fluorescence luminescence resonance energy-transfer molecular beacons. *Anal. Chem*., 75, 15, 3697-3703.
76. Santangelo, P., Nitin, N., Bao, G. (2006) Nanostructured probes for RNA detection in living cells. *Ann. Biomed. Eng*., 34, 1, 39-50.
77. Mhlanga, M.M., Bratu, D.P., Genovesio, A., Rybarska, A., Chenouard, N., Nehrbass, U., Olivo-Marin, J.C. (2009) *In vivo* colocalisation of oskar mRNA and trans-acting proteins revealed by quantitative imaging of the *Drosophila* oocyte. *PLoS One*, 4, 7, e6241.
78. Foe, V.E., Alberts, B.M. (1983) Studies of nuclear and cytoplasmic behaviour during the five mitotic cycles that precede gastrulation in *Drosophila* embryogenesis. *J. Cell Sci.*, 61, 31-70.
79. Zalokar, M. and Erk, I. (1976) Division and migration of nuclei during early embryogenesis of *Drosophila* melanogaster. *Journal of Microbial Cell*, 25, 97–106.
80. Shaila, K., Justin, C., Uyen, T., Blake, R., William, S. (2010) Blastoderm Formation and Cellularisation in *Drosophila* melanogaster. *Encyclopedia of Life Sciences (ELS) John Wiley & Sons, Ltd.*
81. Ip, Y.T., Hemavathy, K. (1997) *Drosophila* development. Delimiting patterns by repression. *Curr. Biol.*, 7, 4, R216-218.
82. Irish, V., Lehmann, R., Akam, M. (1989) The *Drosophila* posterior-group gene nanos functions by repressing hunchback activity. *Nature*, 338, 646 – 648.
83. St. Johnston, D., Nüsslein-Volhard, C. (1992) The origin of pattern and polarity in the *Drosophila* embryo. *Cell*, 68, 2, 201-219.
84. Struhl, G., Johnston, P., Lawrence, P.A. (1992) Control of *Drosophila* body pattern by the hunchback morphogen gradient. *Cell*, 69, 2, 237-249.
85. Tautz, D. (1988) Regulation of the *Drosophila* segmentation gene hunchback by two maternal morphogenetic centres. *Nature*, 332, 281-284.
86. Simpson-Brose, M., Treisman, J., Desplan, C. (1994) Synergy between the hunchback and bicoid morphogens is required for anterior patterning in *Drosophila*. *Cell*, 78, 5, 855-865.

87. Papatsenko, D., Levine, M.S. (2008) Dual regulation by the Hunchback gradient in the *Drosophila* embryo. *Proc. Natl. Acad. Sci. U. S. A.*, 105, 8, 2901-2906.
88. Wreden, C., Verrotti, A.C., Schisa, J.A., Lieberfarb, M.E., Strickland, S. (1997) Nanos and pumilio establish embryonic polarity in *Drosophila* by promoting posterior deadenylation of hunchback mRNA. *Development*, 124, 3015-3023.
89. Martizez, A.A., Baker, N.E., Ingham, P.W. (1988) Role of segment polarity genes in the definition and maintenance of cell states in the *Drosophila* embryo. *Development*, 103, 157-170.
90. Patel, N.H., Schafer, B., Goodman, C.S., Holmgren, R. (1989) The role of segment polarity genes during *Drosophila* neurogenesis. *Genes Dev.*, 3, 890-904.
91. Dinardo, S., O'Farrell, P.H. (1987) Establishment and refinement of segmental pattern in the *Drosophila* embryo: spatial control of engrailed expression by pair-rule genes. *Genes Dev.*, 1, 1212-1225.
92. Gilbert, S.F. (2000) Developmental Biology. 6th edition, Sinauer Associates, Inc.

Chapter 1

The detection of RNA expressed in *Drosophila* embryo with pyrene modified RNA probes

1.1 Introduction

Recent RNA research has revealed the close involvement of various RNAs in cellular functions. Not only RNA itself, but also RNA protein complexes such as miRISC are key players in cells [1]. RNA has been becoming the inevitable target molecules for research of gene expression in details. In order to clarify the roles of RNA related molecules, Northern blotting [2], RT-PCR [3], and DNA microarray [4] have been included in many conventional studies. However, those techniques cannot study the differences between individual cells, tissues and embryos. In tissues, the individual cells may present different gene expressions. In embryos, the cells may be in different stages of differentiation. Therefore, new systems for the observation of gene expressions in individual cells are necessary.

RNA and its related complexes are also promising targets for disease diagnosis [5, 6]. Multi-cellular specimens such as organ tissues, histopathological specimens, and embryos are among the possible targets of RNA-based diagnostic techniques. Proof of the presence of certain RNAs in a specimen could provide information about diseases such as SARS [7] and newly emerging virus infections [8]. Rapid and possibly quantitative analysis of a specific RNA could easily lead to rapid and precise diagnosis of diseases. Taking this background into consideration, both in research into fundamental biology and in clinical disease diagnosis, selective and rapid detection of specific RNA in multi-cellular specimens is essential. The conventional analytical method of RNA is *in situ* hybridization accompanied with an immune staining protocol, which requires cDNA having a certain antigen such as digoxigenin and biotin [9]. Though this protocol has shown reliability to date, it requires skills and time-consuming procedures. Recently, elegant *in situ* hybridization protocols to detect RNA and its

related substances have been reported [10-12]. That is, RNA imaging protocols have been intensively developed using fluorescent nucleic acid probes, and the rapid development of imaging technology has accelerated this field, allowing the visualization of RNA in cells, tissues and embryos. Several reports related to this new protocol include molecular beacons [13, 14], FRET-probes [14, 15], quenched autoligation probes [16], and fluorescent-protein based probes [17]. Though the probes used in those detection protocols have presented promising results for gene imaging studies, they were not RNA specific. For further development of RNA detection systems for the diagnosis of diseases, detection systems that can clearly detect RNA in specimens are urgently required.

A unique fluorescent RNA-specific probe having two consecutive pyrene-conjugated pyrimidine nucleosides has been developed. A pyrene was introduced at the 2'-position of a pyrimidine nucleoside denoted as Upy. Our probe, 2'-*O*-methyloligoribonucleotides (2'OMe ORN) having two consecutive modified nucleosides, denoted as OMUpy2, possesses two important characteristics. First, it is highly RNA specific [18, 19]. The hybrids between OMUpy2 and its complementary oligo RNA (cORN) are highly fluorescent, whereas those between OMUpy2 and its complementary DNA are scarcely fluorescent. Even the hybrids between OMUpy2 and cORN containing a single mismatch cause significant quenching of the fluorescence. The spectroscopic studies revealed that the fluorescent behavior of the pyrene attached to the sugar was strongly affected by the surrounding environment of the pyrene [20]. And conformational studies using molecular dynamic simulations and 1H NMR measurements revealed that the pyrene attached to the sugar in an RNA duplex was located outside of the helix, whereas that in a DNA duplex was located inside of the helix [21]. Therefore, the pyrene modified RNA provides a useful tool for RNA detection. Secondly, OMUpy2 does not emit fluorescence alone when excited. Therefore, a washing procedure to remove unbound probes from the detection system is not necessary, which enables the application of the probes to *in situ* RNA detection in living cells.

In the present study, we conducted *in situ* RNA detection in multi-cellular

systems, *Drosophila* embryo, using OMUpy2. This system is suitable for detecting RNA in its spatial and temporal aspects, because it is easy to evaluate whether the probe was able to detect the RNA target from the position of RNA expression changing according to the kinds of RNA and development time. In addition, the protocol employed in this study makes whole mount *in situ* hybridization (WISH), which is commonly used for embryo studies, easier and faster than ever due to the elimination of washing steps. We especially focused on Krüppel mRNA (Kr mRNA). The Krüppel gene, a gap gene, is one of the first zygotic segmentation genes activated in early *Drosophila* embryos [22, 23]. It is well known that the Kr mRNA is abundantly expressed in the early stages of differentiation, and its temporal and spatial expression patterns have been well characterized [24-26]. Transcription of Kr mRNA starts at the syncytial blastoderm stage (stage-3) and lasts up to 8 h after fertilization [27]. At the onset of transcription, the Kr mRNA is detected mostly in the center domain of *Drosophila* embryos during stage-3-5 [9, 25, 26]. Therefore, OMUpy2 for Kr mRNA is expected to emit signals in the center region of *Drosophila* embryos if it specifically hybridizes with Kr mRNA in the embryos.

1.2 Materials and Methods

1.2.1. Probe preparation

The probes were synthesized according to previous reports using conventional phosphoramidite chemistry and purified by reversed-phase HPLC [28]. The sequences used in this study are listed in Table 1. Kr-F is a 5'-fluorescein labeled 2'-OMe ORN which has the same nucleotide sequence as Kr-OMUpy2. Kr-OMUnonpy is a non-pyrene-labeled 2'-OMe ORN which has the same sequence as Kr-OMUpy2. Control-OMUpy2 consists of the same base composition as Kr-OMUpy2 with a scrambled sequence.

1.2.2. The extraction of total RNA from *Drosophila* embryos and purification of mRNA

All embryos used in this study were from wild-type *Drosophila* flies (Canton S). Embryos were collected at 2-hour intervals and aged until the desired developmental stage on yeast juice agar plates at 25 °C. The embryos were dechorionated with 5 % sodium hypochlorite in water for 1.5 min and then frozen in liquid nitrogen. After 500 µl of TRIzol® Reagent (Invitrogen) was added to the frozen embryos on ice, the embryos were homogenized quickly, and further 500 µl TRIzol® Reagent and 200 µl chloroform/isoamyl alcohol (49/1, v/v) were added, followed by vigorous shaking. After incubation on ice for 5 min, the suspension was centrifuged at 12,000 rpm at 4 °C for 15 min. RNA in the aqueous phase was transferred to a sterilized tube. After addition of 500 µl of isopropanol to the tube, the solution was stored on ice for 5 min followed by centrifugation at 12,000 rpm at 4 °C for 10 min. Isopropanol was exchanged with 75 % aq. ethanol and the ethanol solution was centrifuged at 7,500 rpm at 4 °C for 3 min three times. The precipitate, RNA, was suspended in 75 % aq. ethanol and stored at -20 °C for more than 12 hours. The RNA suspension was collected by centrifugation and dissolved in PBS buffer, followed by treatment with an oligo (dT)-cellulose column (GE Healthcare).

1.2.3. Fluorescence measurements

Fluorescence spectra were measured with a spectrofluorophotometer (RF-5300PC, Shimadzu). The fluorescence spectra of Kr-OMUpy2 in the presence of the extracted mRNA were measured with a micro volume cell (Capillary Adaptor Cell; HELIX Biomedical Accessories; cell volume, 3 µl). The concentration of the extracted mRNA solution used for measurements was 65 mg/ml and those of Kr-OMUpy2 and Control-OMUpy2 were each 30 µM.

1.2.4. Whole mount *in situ* hybridization

The collections of *Drosophila melanogaster* wild-type embryos, Canton S, were dechorionated in a solution of 5 % sodium hypochlorite in water for about 1.5 min in a small basket. Embryos were thoroughly washed with 0.07 % NaCl/ 0.1 % TritonX-100. The embryos were then fixed with 4 % paraformaldehyde in 10 mM phosphate buffer containing 0.1 M NaCl and heptane (1/4 : v/v) with gentle shaking for 20 min at 25 °C. After fixation, the aqueous phase was completely removed and embryos were vigorously shaken in a 1:1 mixture of heptane and methanol so that they were devitellinized. Embryos were then washed with methanol twice and stored in 100 % methanol at -85 °C [29]. Prior to WISH using fixed embryos, the supernatant, methanol, was sequentially exchanged with PBT (10 mM phosphate buffer, pH 7.0/ 0.1 M NaCl/ 0.1 % Tween 20) /methanol solution (75, 50, and 25 % methanol) and then washed twice in PBT. Embryos were stored in PBT at 25 °C for 15 min. The fixed embryos were then added in the probe solution (30 µM OMUpy2 in PBT), followed by incubation at 40 °C for 30 min, then at 4 °C for 2 hours. The embryos treated with probes were then washed with PBT once. Embryos were mounted on a glass slide in 70 % glycerol in PBS and observed by fluorescent microscope using a 20 × objective lens.

1.2.5. Microscopic measurement and photography

Microscopic measurements and imaging of embryos treated with OMUpy2 were performed on a Nikon ECLIPSE TE300 (Nikon) microscope equipped with a xenon lamp. Fluorescent images were obtained under the following conditions: Filter sets: For OMUpy2, EX: 340/15 nm, DM: 380 nm, EM: 480/30 nm; For Kr-F, EX: 470/20 nm DM: 505 nm EM: 535/25 nm. The objective lens was a 20 ×/0.45 Plan Fluor (Nikon) for differential interference contrast (DIC) images. The merge images were converted to pseudo-color. Microscopic fluorescence spectra were measured with a Hamamatsu photonic multi-channel analyzer (PN-100, Hamamatsu Photonics, Hamamatsu) under the following conditions: EX: 340/15 nm DM: 380 nm. The exposure time for obtaining images was 1 sec and that for obtaining spectra was 5 sec.

Results and Discussion

1.3.1. Probe preparation

RNA specific probes containing two consecutive pyrene-conjugated nucleotides (OMUpy2) were synthesized according to previous reports [18]. The structure of the core region in OMUpy2 and typical fluorescence spectra of bispyrene and monopyrene are shown in Figure 1. The target site for OMUpy2 must satisfy the following three points. The first is the sequences of target RNA need to contain ApA sequence, where UpyUpy in OMUpy2 can hybridize. Second, the base followed by UpyUpy must be a pyrimidine base as to form an environment in which pyrene emits excimer, namely the base followed by ApA mast be a purine base. Third, the target sites have high potential to form a single-stranded region.

The nucleotide positions chosen as the target site for OMUpy2 were based on the results of Loop Probability value (LP value) (Figure 2.) taking into account the conditions described above. Loop Probability represents the accessibility of probe to each base. Each base belongs to a part of the loop structure or stem structure in the folding RNA. Its belonging changes depending on the state of the folding RNA. For each base, the probability to form a loop structure was calculated from secondary RNA structure based on the software, “RNA Structure 4.6”, Mathews *et al.* [30, 31] developed by the thermodynamic methods which are based on nearest neighbor rules that predict the stability of a structure quantified by folding free energy change [30, 32, 33]. In brief, Loop Probability value (LP value) of the base which can always form a loop structure shows LP value=1. LP value of the base which always forms a stem structure shows LP value=0. LP value is an average calculated based on twenty RNA secondary structures which were predicted in ascending order of energy [34]. The entire sequences were scanned sequentially for secondary structure formation in contiguous frames of 100 bases. the frames for the simulation of secondary structures were staggered down by 30 bases, resulting in an overlap of 70 bases on the 5’ side of the second set of fram (100 nt frame-30 nt shift). This procedure is repeated many times so that any given sequences are scanned for its potential secondary structure in other

different frames. LP value was calculated from three types of RNA secondary structures, 100 nt frame-30 nt shift, 300 nt frame-100 nt shift, and 700nt frame (Figure 2a-g.). Details of RNA probes and ORNs used in the present study are shown in Table 1.

As a backbone of OMUpy2, 2'-*O*-methyl RNA was employed because they have high stability in terms of its enzyme resistance and the affinity with ORN. 2'-*O*-methyl RNA also permits selective binding at 37 °C [35-40].

(1) (2)

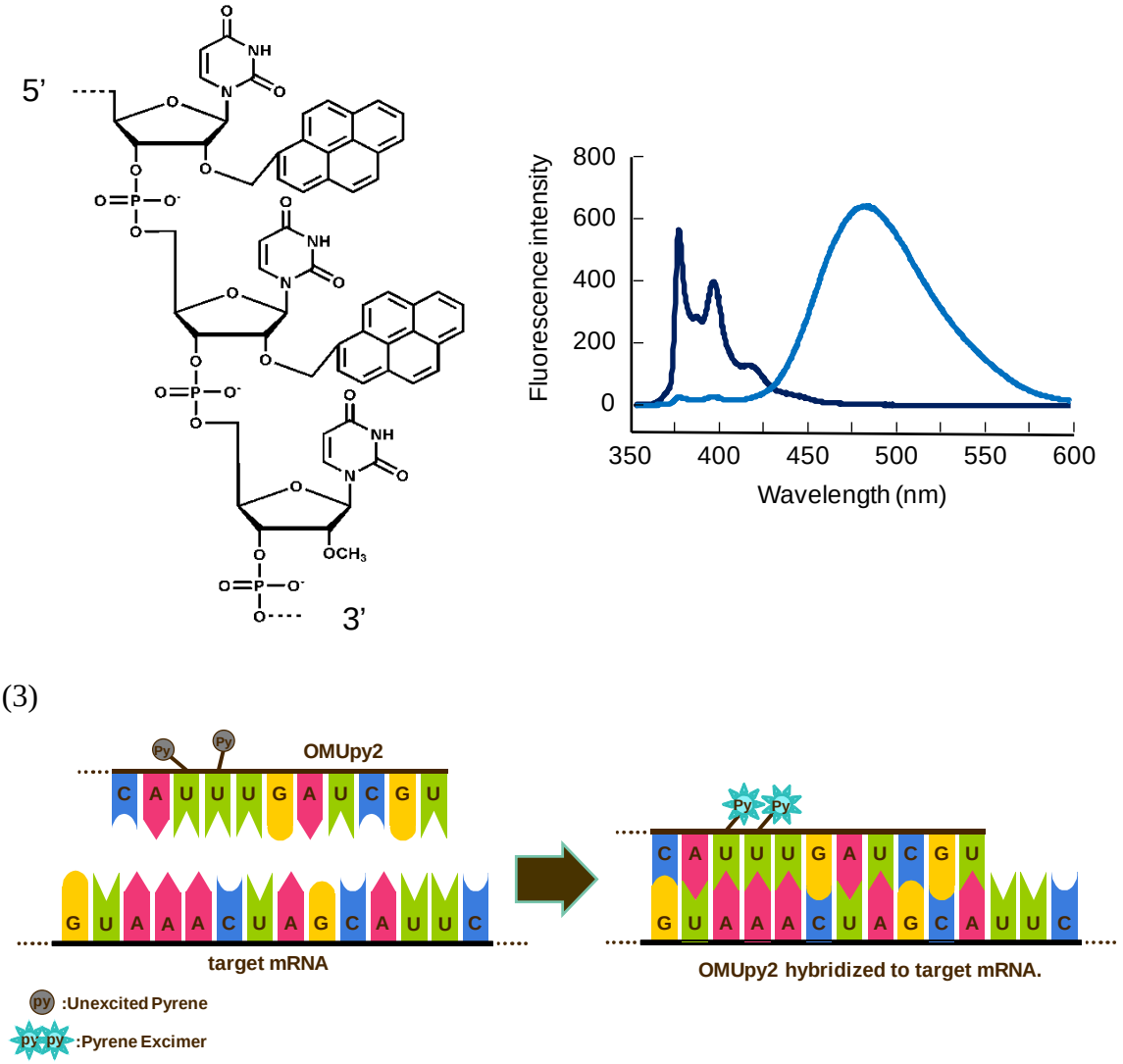

(3)

Figure 1. (1) The structure of the core region in OMUpy2. (2) Fluorescence spectra of bispyrene and monopyrene. (3) Scheme of OMUpy2.

(2) light blue: bispyrene, dark blue: monopyrene. λex = 342 nm. (3) OMUpy2 emits fluorescence at around 480 nm only when it binds to complementary RNA.

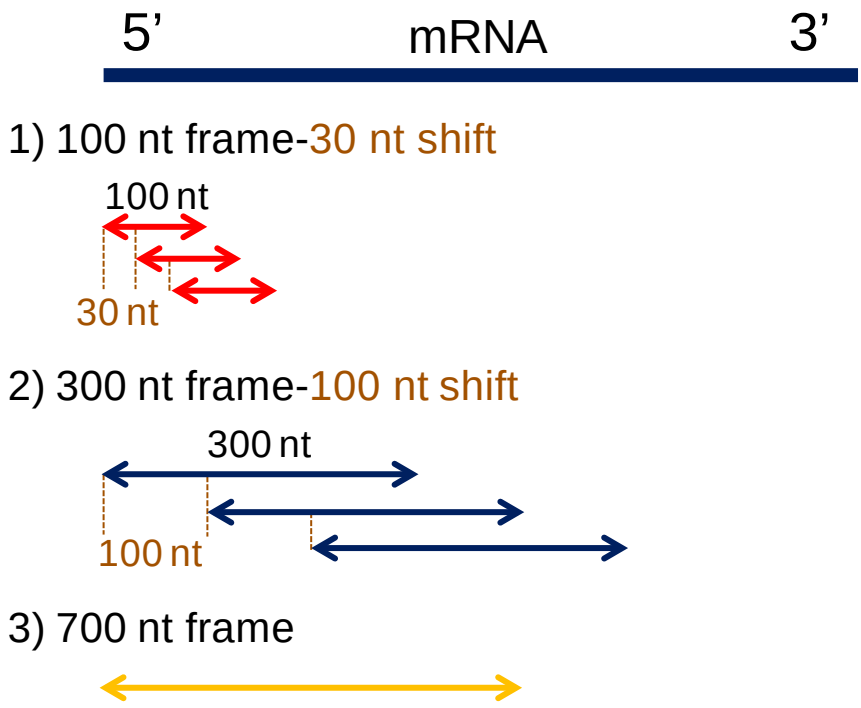

Figure 2a. A method of predicting RNA secondary structure to calculate the LP value.

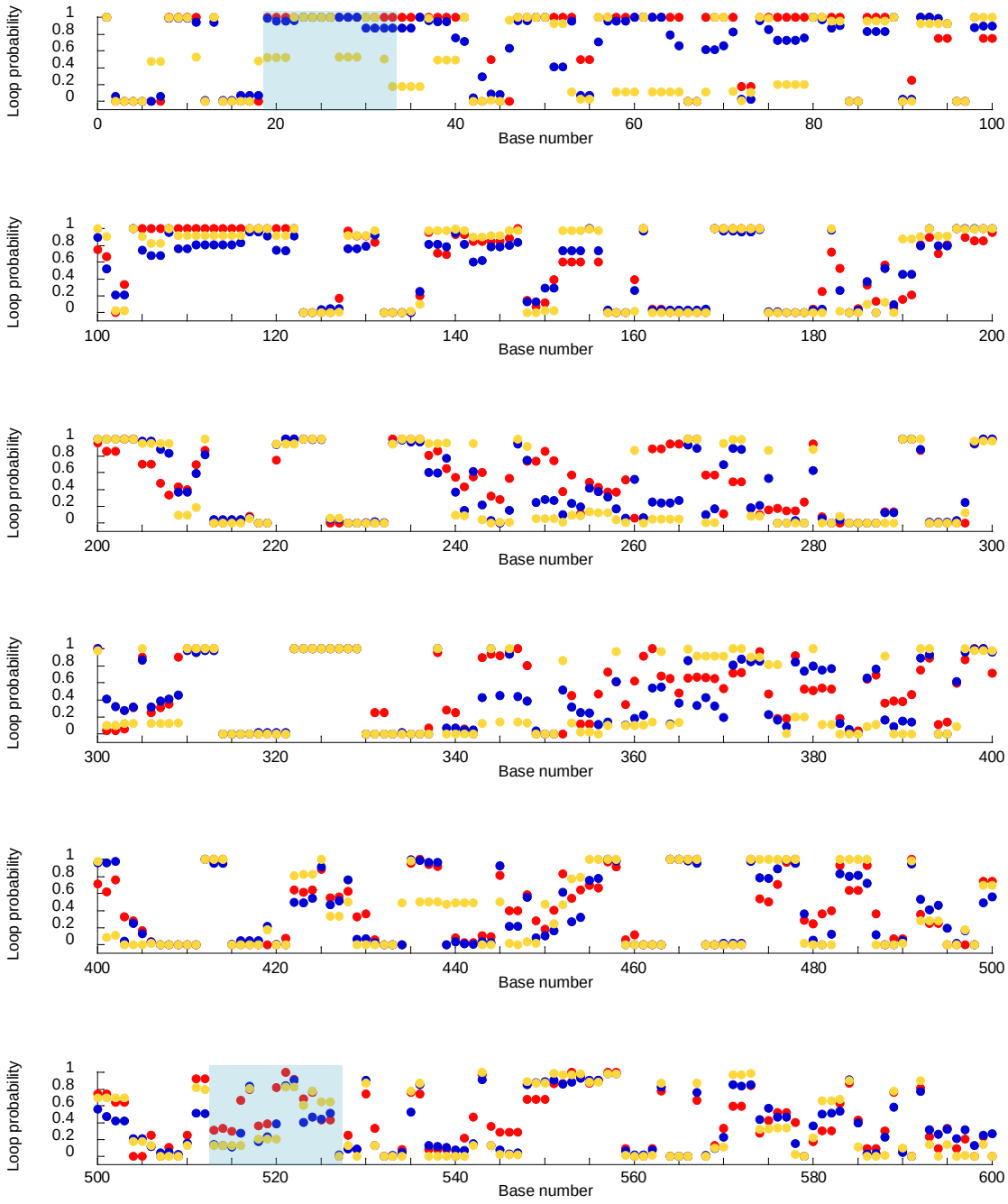

Figure 2b. Loop probability values of bicoid mRNA.

red: 100 nt frame 30nt shift, blue: 300 nt frame 100 nt shift, yellow: 700 nt frame. The target sites are painted in blue. The details of sequences are presented in Table 1.

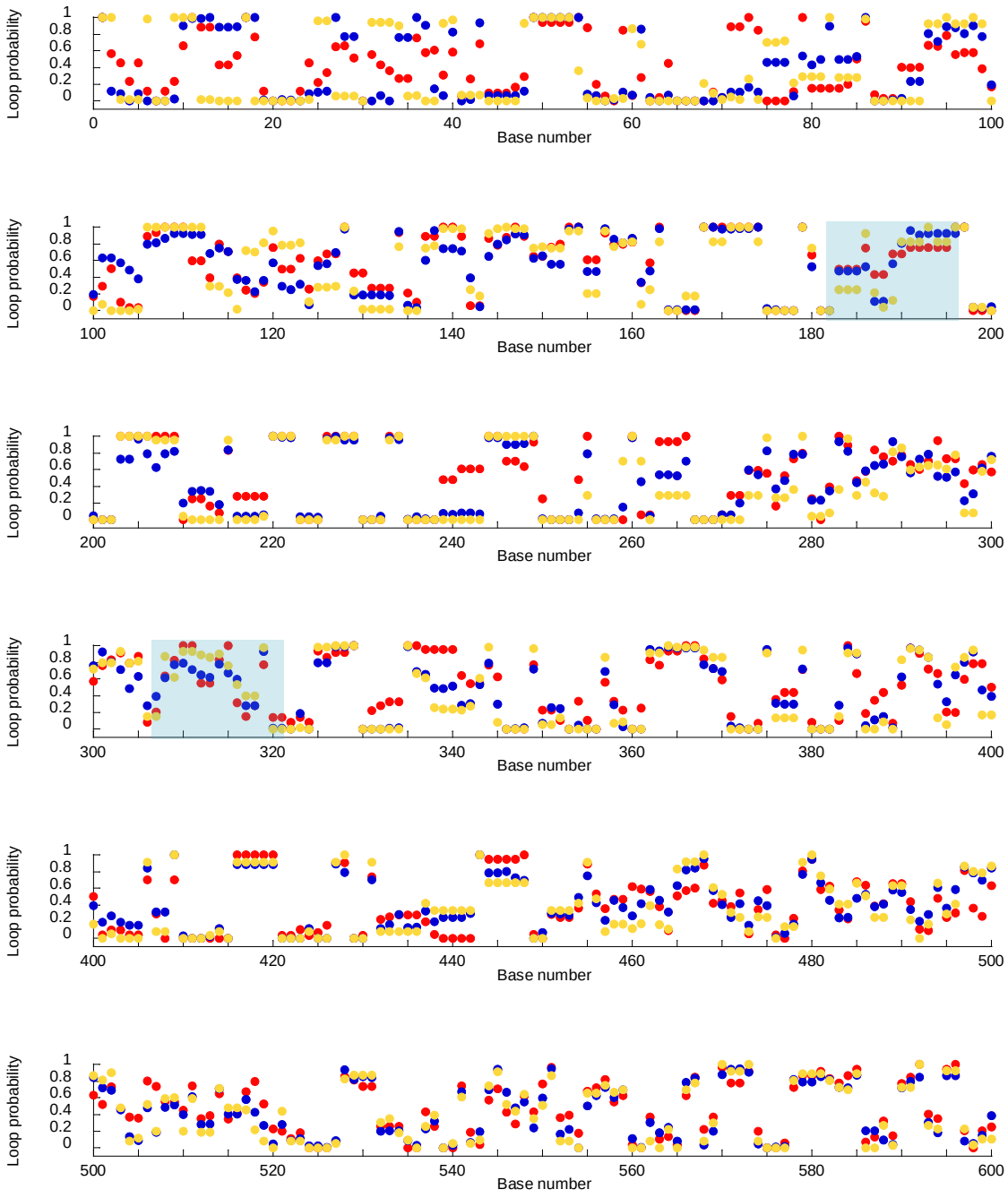

Figure 2c. Loop probability values of even-skipped mRNA.

red: 100 nt frame 30nt shift, blue: 300 nt frame 100 nt shift, yellow: 700 nt frame. The target sites are painted in blue. The details of sequences are presented in Table 1.

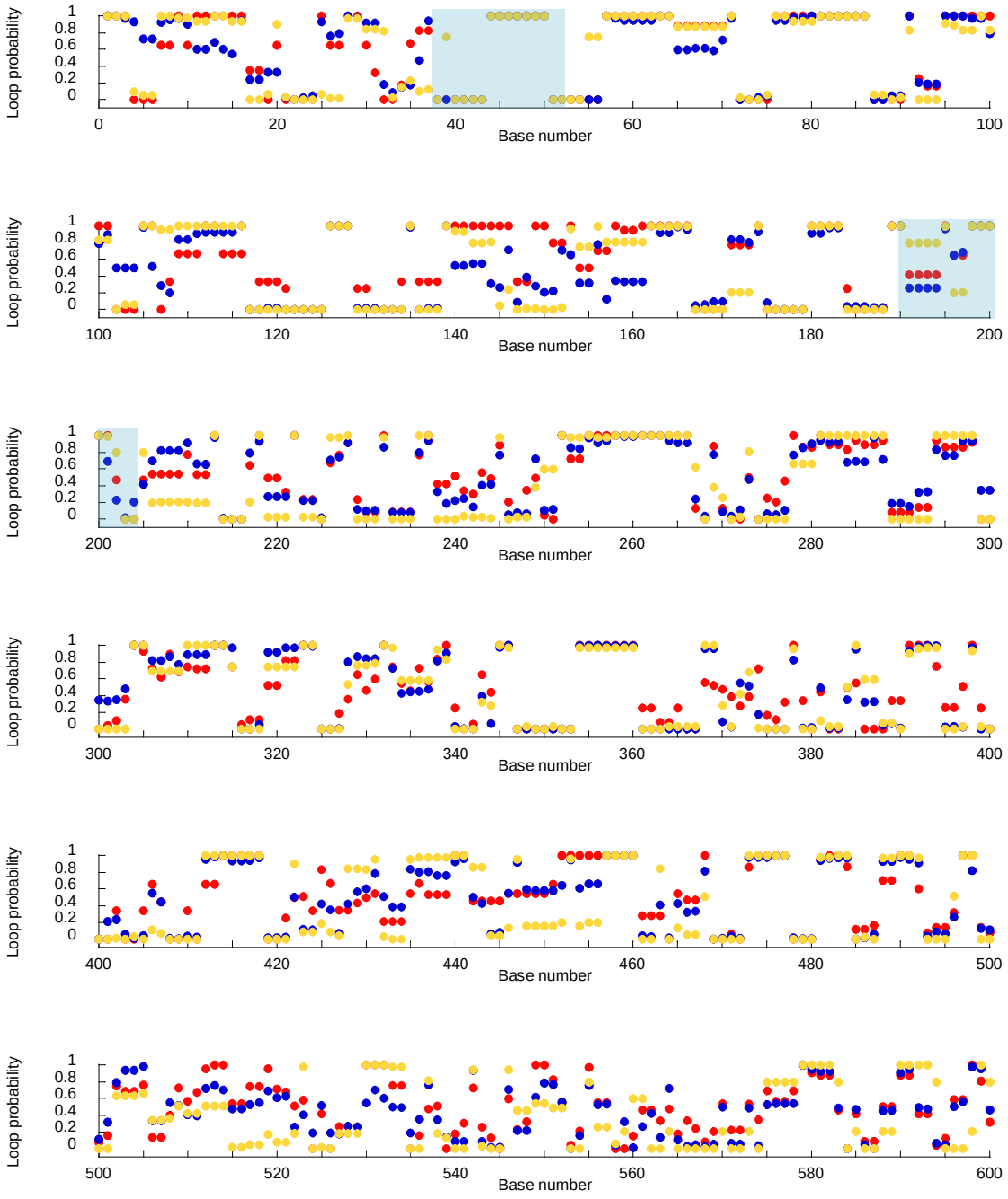

Figure 2d. Loop probability values of fushi-tarazu mRNA.

red: 100 nt frame 30nt shift, blue: 300 nt frame 100 nt shift, yellow: 700 nt frame. The target sites are painted in blue. The details of sequences are presented in Table 1.

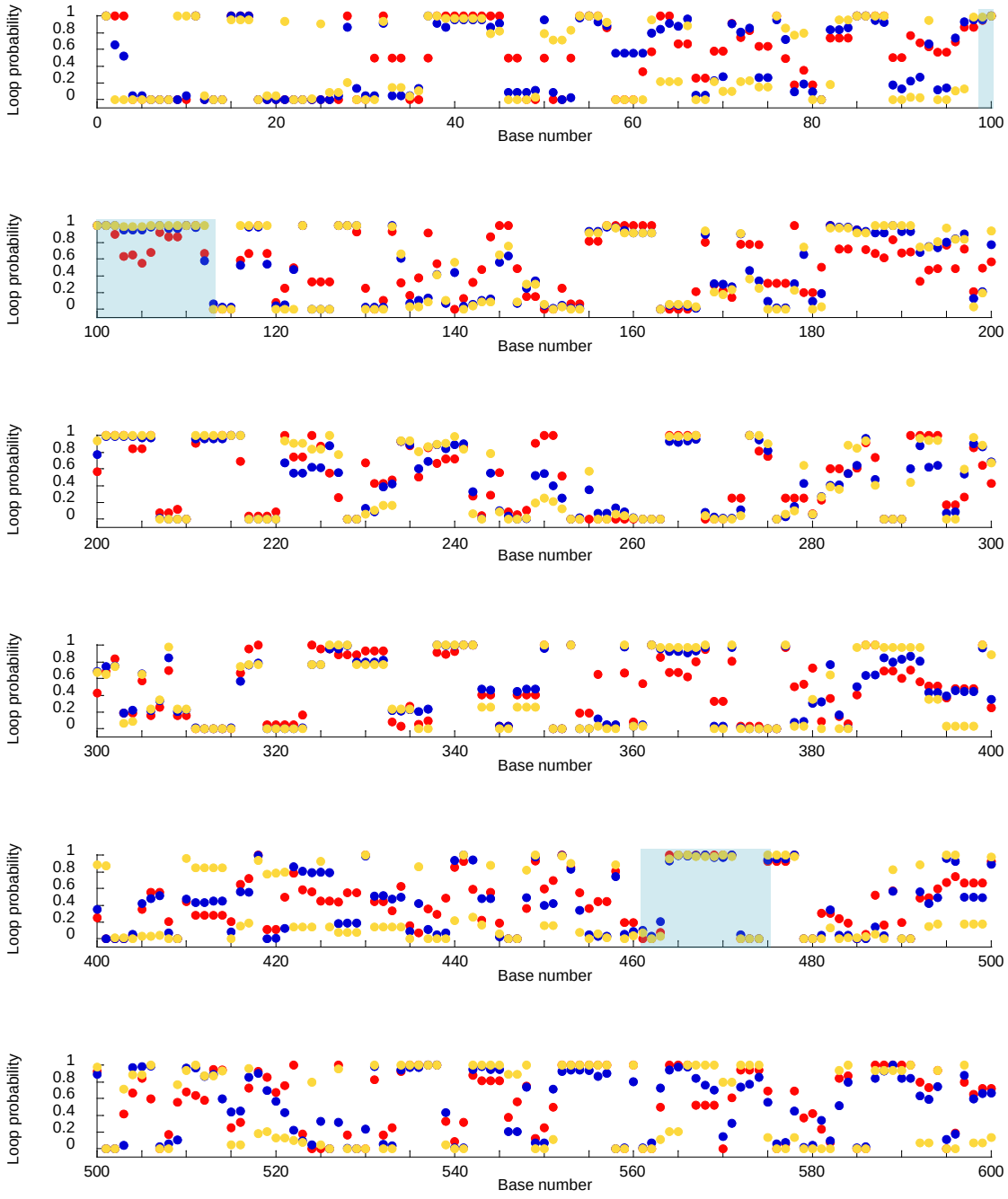

Figure 2e. Loop probability values of giant mRNA.

red: 100 nt frame 30nt shift, blue: 300 nt frame 100 nt shift, yellow: 700 nt frame. The target sites are painted in blue. The details of sequences are presented in Table 1.

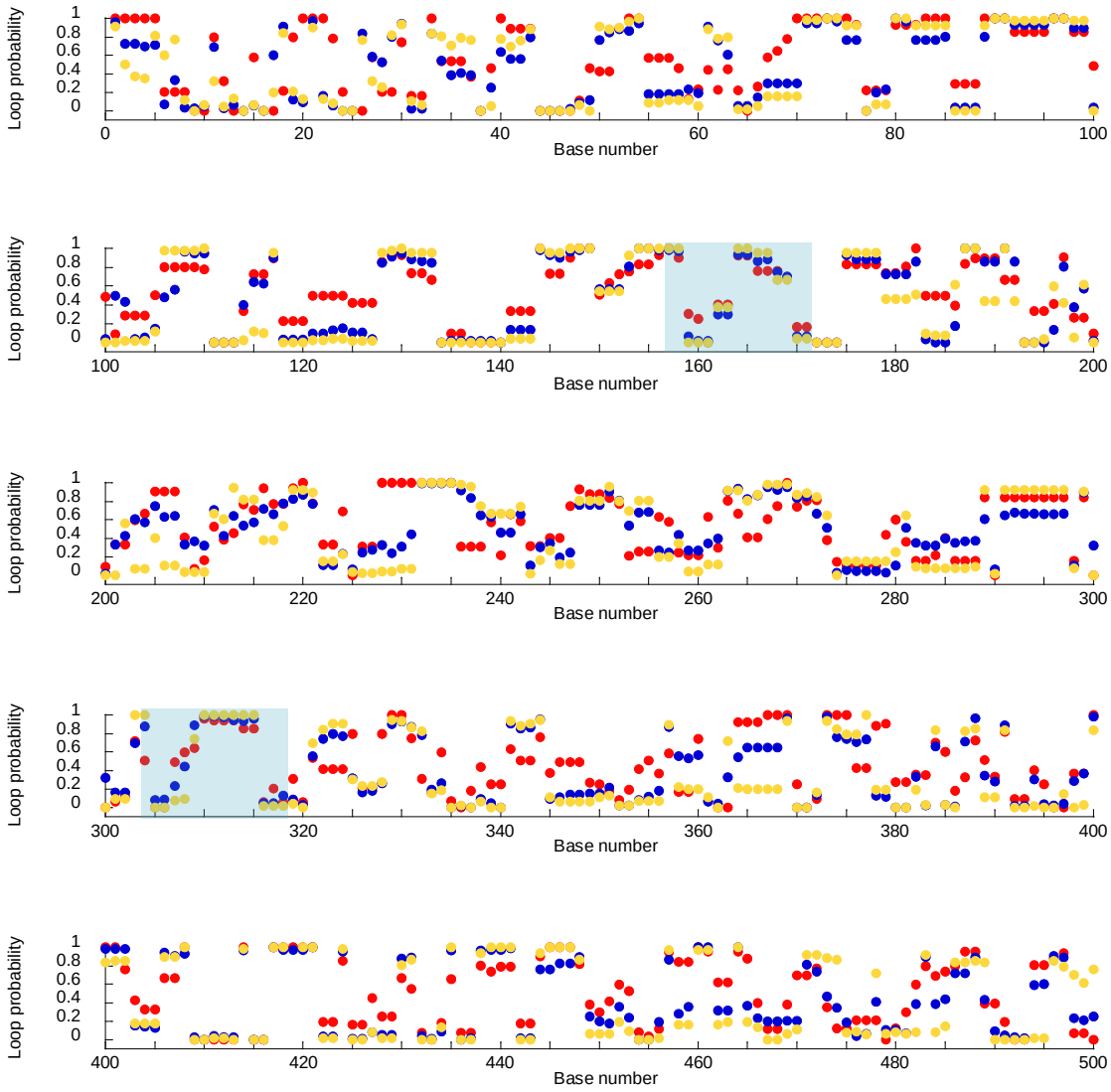

Figure 2f. Loop probability values of Krüppel mRNA.

red: 100 nt frame 30nt shift, blue: 300 nt frame 100 nt shift, yellow: 700 nt frame. The target sites are painted in blue. The details of sequences are presented in Table 1.

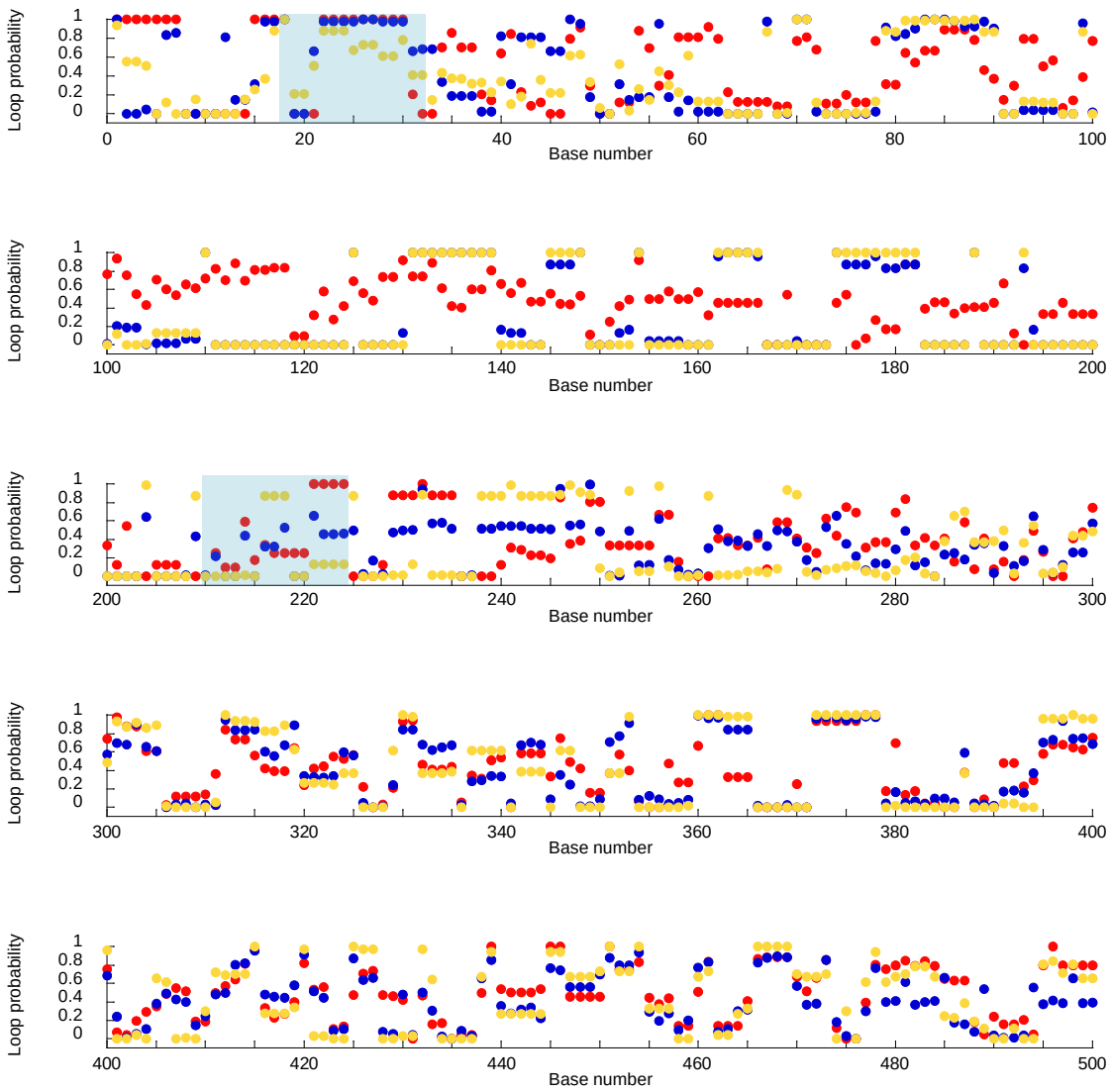

Figure 2g. Loop probability values of nanos mRNA.

red: 100 nt frame 30nt shift, blue: 300 nt frame 100 nt shift, yellow: 700 nt frame. The target sites are painted in blue. The details of sequences are presented in Table 1.

Table 1. Sequences used in the present study.

RNA target	name	5’ SEQUENCES 3’ upper: target RNA / lower: probe	Nucleotide positions	GenBank ID/ miRBase Accession
bicoid mRNA	bcd1-ORN	GAU CAA AAC UUU UAC	19-33	7646
	bcd1-OMUpy2	*GUA AAA G*UpyUpy *UUG AUC*		
	bcd2-ORN	GGG UAU GAA ACA GAG	513-527	
	bcd2-OMUpy2	*CUC UGU* UpyUpy*C AUA CCC*		
even-skipped mRNA	eve1-ORN	GAU ACC GAA CCU ACA	182-196	45549169
	eve1-OMUpy2	*UGU AGG* UpyUpy*C GGU AUC*		
	eve2-ORN	CCA AAU GAA UGC CUA	307-321	
	eve2-OMUpy2	*UAG GCA* UpyUpy*C AUU UGG*		
fushi-tarazu mRNA	ftz1-ORN	GUU AGA GAA GAA AUC	38-52	19549961
	ftz1-OMUpy2	*GAU UUC* UpyUpy*C UCU AAC*		
	ftz2-ORN	CUA UCA GAA CAC CUC	190-204	
	ftz2-OMUpy2	*GAG GUG* UpyUpy*C UGA UAG*		
giant mRNA	gt1-ORN	UAC ACC GAA CAC CAU	99-113	24639344
	gt1-OMUpy2	*AUG GUG* UpyUpy*C GGU GUA*		
	gt2-ORN	CGU AUC AAA CAA GCU	461-475	
	gt2-OMUpy2	*AGC UUG* UpyUpy*U GAU ACG*		
Krüppel mRNA	Kr-ORN	AGC ACA AAA UUA GGA	304-318	22024037
	Kr-OMUpy2	*UCC UAA* UpyUpy*U UGU GCU*		
	Kr-F	F-*UCC UAA UUU UGU GCU*		
	Kr-OMUnonpy	*UCC UAA UUU UGU GCU*		
	Control-OMUpy2	*AGU CAC* UpyUpy*U UUC GUU*		
	Kr2-ORN	AAG UAC AAA AGU GUG	157-171	
	Kr2-OMUpy2	*CAC ACU* UpyUpy*U GUA GUU*		
nanos mRNA	nos1-ORN	ACC ACA AAA UUC CUG	18-32	24648141
	nos1-OMUpy2	*CAG GAA* UpyUpy*U UGU GGU*		
	nos2-ORN	UUG UGG AAA GUA GAG	210-224	
	nos2-OMUpy2	*CUC UAC* UpyUpy*U CCA CAA*		
28S rRNA	28S-ORN	CGCUCAUCAGACCCCAGAAAAG	1903-1924	337381
	28S-OMUpy2	*CUU UUC UGG GG*Upy Cpy*UG AUG AGC G*		
hsa-mir-21	miR21-ORN	UAG CUU AUC AGA CUG AUG UUG A	8-29	MI0000077
	miR21-OMUpy2	*UCA ACA UCA G*UpyCpy *UGA UAA GCU A*		
hsa-mir-24-2	miR24-ORN	UGG CUC AGU UCA GCA GGA ACA G	50-71	MI0000081
	miR24-OMUpy2	*CUG UU*Cpy Cpy*UG CUG AAC UGA GCC A*		

Italic letters: 2’-OMe nucleotides, capital letters: ribonucleotides.
Upy: 2’-*O*-pyrenylmethyluridine, Cpy: 2’-*O*-pyrenylmethylcytidine
Kr-F: 5’-fluorescein-labeled probe with same sequence as Kr-OMUpy2.
Kr-OMUnonpy: non-pyrene-labeled probe with the same sequence as Kr-OMUpy2.
Control-OMUpy2: scrambled sequence with the same base composition as Kr-OMUpy2.
28S-ORN: the sequence complementaery to nucleotide positions (1903-1924) in *Human* 28S ribosomal RNA gene.

1.3.2. Fluorescence spectra of Kr-OMUpy2 and Control-OMUpy2 in the presence and absence of Kr-ORN

Fluorescence spectra of Kr-OMUpy2 in the presence and absence of the complementary ORN (Kr-ORN) and oligo DNA (Kr-ODN) are shown in Figure 3a. While the equimolar solution of Kr-OMUpy2 and Kr-ORN emitted the fluorescence peaked at around 480 nm, the fluorescence of the equimolar solution of Kr-OMUpy2 and Kr-ODN was hardly observed. The spectrum showed the typical fluorescence of bispyrene and these results were in accord with a previous report. Little to no fluorescence around 480 nm from Kr-OMUpy2 itself, Control-OMUpy2 itself, and the equimolar solution of Control-OMUpy2 and Kr-ORN were observed (Figure 3b.). In addition, we also observed little emission around 480 nm from the equimolar solution of Kr-OMUpy2 and noncomplementary ORNs (28S-ORN, miR24-ORN, and miR21-ORN) (Figure 3c.). These results indicate that 15-nt Kr-OMUpy2 has sufficient sequence specificity to identify complementary sequences because it did not fluorescence almost around 480 nm unless in the presence of its complementary RNA, Kr-ORN. Based on a previous report [18], we attributed the fluorescence around 480 nm to a pyrene excimer formed by a hybrid formation between OMUpy2 and its complementary RNA.

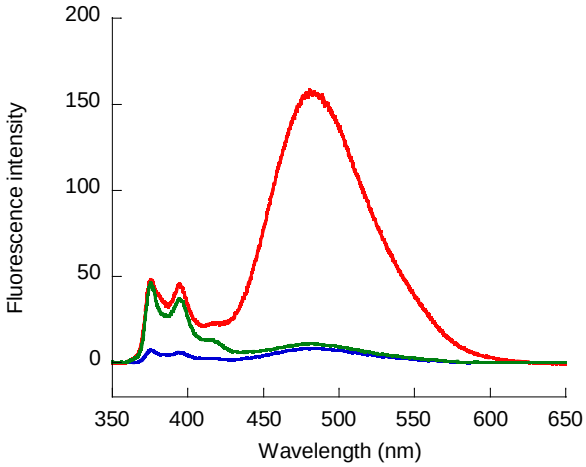

Figure 3a. Fluorescence spectra of Kr-OMUpy2 in the presence of Kr-ORN and Kr-ODN.

red line: Kr-OMUpy2/Kr-ORN, blue line: Kr-OMUpy2, green line: Kr-OMUpy2/Kr-ODN, [Kr-OMUpy2] = [Kr-ORN] = [Kr-ODN] = 0.75 μM, 10 mM phosphate buffer (pH 7.0) containing 100 mM NaCl, 11 °C, λex = 342 nm.

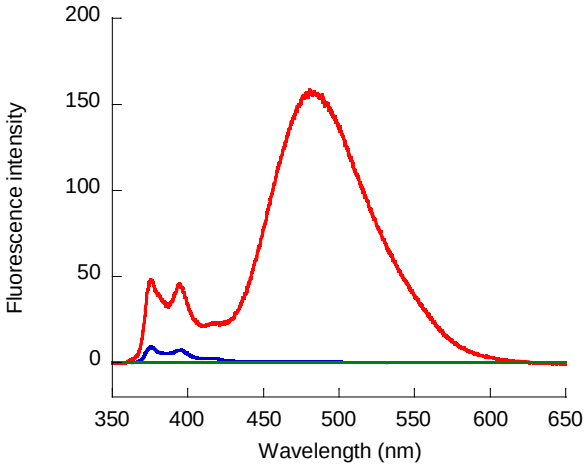

Figure 3b. Fluorescence spectra of Kr-OMUpy2 and Control-OMUpy2 in the presence and absence of Kr-ORN.

red line: Kr-OMUpy2/Kr-ORN, blue line: Control-OMUpy2/Kr-ORN, green line: Control-OMUpy2, [Kr-OMUpy2] = [Control-OMUpy2] = [Kr-ORN] = 0.75 μM, 10 mM phosphate buffer (pH 7.0) containing 100 mM NaCl, 11 °C, λex = 342 nm.

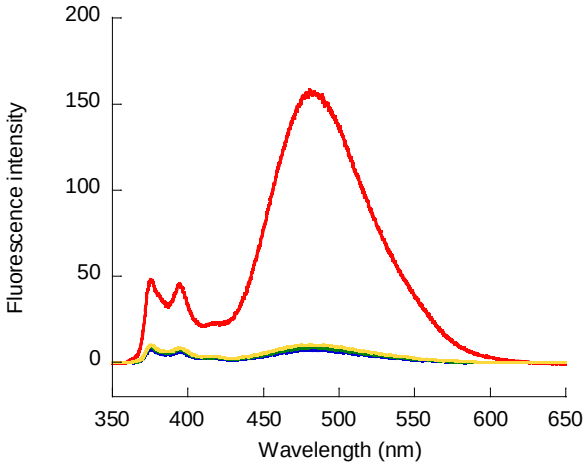

Figure 3c. Fluorescence spectra of Kr-OMUpy2 in the presence of noncomplementary ORN

red line: Kr-OMUpy2/Kr-ORN, blue line: Kr-OMUpy2/28S-ORN, yellow line: Kr-OMUpy2/miR21-ORN, green line: Kr-OMUpy2/miR24-ORN, [Kr-OMUpy2] = [Kr-ORN] = [28S-ORN] = [miR21-ORN] = [miR24-ORN] = 0.75 μM, 10 mM phosphate buffer (pH 7.0) containing 100 mM NaCl, 11 °C, λex = 342 nm.

1.3.3. The linear relationship between fluorescence intensity of OMUpy2 and the concentration of ORN

In order to evaluate the capability of OMUpy2 in terms of the quantitative detection of RNA, the fluorescence intensity of OMUpy2 in the presence of the complementary ORN (cORN) was measured in the range of 10 nM to 1000 nM cORN concentration. The fluorescence intensity at 480 nm of OMUpy2-cORN hybrids versus the concentration of cORN had a linear relationship at the range of 10 nM to 1000mM as shown in Figure 4. This result shows that OMUpy2 is able not only to detect the RNA target at the range of 10 nM to 1000mM, but also to evaluate the amount of the RNA target from the fluorescence intensity.

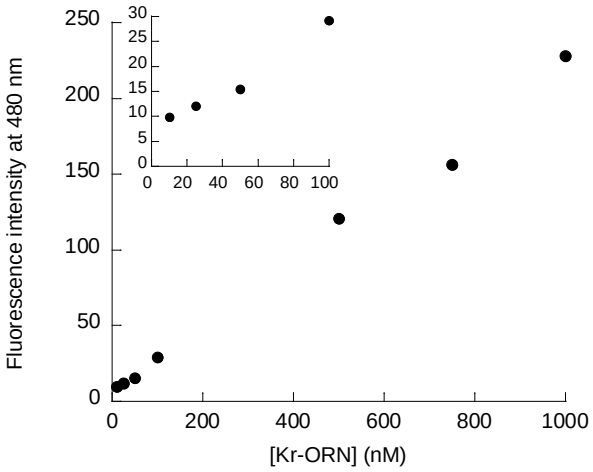

Figure 4. The linear relationship between fluorescence intensity of OMUpy2 and the concentration of ORN.

[Kr-OMUpy2] = 1000 nM, [Kr-ORN] = 10 nM-1000 nM, 10 mM phosphate buffer (pH 7.0) containing 100 mM NaCl, λex = 340 nm, λem = 480 nm.

1.3.4. The detection of target RNA in total RNA extracted from *Drosophila* embryos using OMUpy2

Although Mahara *et al*. [18] revealed that the 15-nt OMUpy2 bound to 120-nt *E. coli* 5S-rRNA, this does not necessarily mean that the OMUpy2 can recognize the complementary sequence in the longer target mRNA such as 2500-nt Kr mRNA under the presence of many other RNAs. We therefore measured emission spectra of the Kr-OMUpy2 solution and the Control-OMUpy2 solution, respectively, both of which were added to the extracted mRNA purified through total RNA from *Drosophila* embryo by the oligo dT cellulose column. Total mRNA (3-5-hr mRNA) was extracted from 3-5-hr embryos expressing Kr mRNA. Kr-OMUpy2/3-5-hr mRNA solution and Control-OMUpy2/3-5-hr mRNA solution were concentrated into two microliters and their fluorescence characteristics were measured with a microvolume capillary adaptor cell. As a result, Kr-OMUpy2/3-5-hr mRNA solution showed an emission at around 480 nm. However, Control-OMUpy2/3-5-hr mRNA solution did not emit signals (Figure 5a.). The complementary sequence to the core region of Control-OMUpy2, CUpyUpyUU, is included in eight places of Kr mRNA and in five places of them, six consecutive bases are corresponding to a part of Kr mRNA. This means that OMUpy2 has the high sequence selectivity and was more likly to bind to the target part of Kr mRNA.

To further confirm that the emission from Kr-OMUpy2 probe/3-5-hr mRNA solution was attributed from the specific binding of Kr-OMUpy2 to Kr mRNA, the spectrum of the solution of Kr-OMUpy2/0-2-hr mRNA extracted from embryos before Kr mRNA colud be expressed abundantly was measured. The fluorescence intensity at 480 nm of Kr-OMUpy2/0-2-hr mRNA solution decreased to 25 % compared to that of the Kr-OMUpy2/3-5-hr mRNA solution (Figure 5a.). These results indicate that Kr-OMUpy2 is capable of selectively detecting Kr mRNA in the solution containing various RNAs, RNA pool.

To verify whether the emission in Kr-OMUpy2/0-2-hr mRNA solution was attributed to sequence specific hybridization of Kr-OMUpy2 with the targeted sequence in Kr mRNA, we performed a competition assay using Kr-OMUnonpy whose sequence

was the same as that of Kr-OMUpy2 except for the absence of two consecutive pyrenes. Tm values of Kr-OMUpy2 and cORN duplex and Kr-OMUnonpy and cORN duplex are 60 ˚C and 65 ˚C, respectively. The addition of Kr-OMUnonpy to the solution of Kr-OMUpy2/0-2-hr mRNA caused the large reduction of the fluorescence intensity at around 480 nm (Figure 5b.). It suggests that Kr-OMUpy2 recognized Kr mRNA in a sequence-specific manner and succeeded in detecting Kr mRNA.

To investigate relative RNA expression levels, bcd1-OMUpy2, bcd2-OMUpy2, nos1-OMUpy2, nos2-OMUpy2, gt1-OMUpy2, gt2-OMUpy2, Kr-OMUpy2, Kr2-OMUpy2, ftz1-OMUpy2, ftz2-OMUpy2, eve1-OMUpy2, and eve2-OMUpy2 were respectively added to total RNA extracted from 0-9-hr *Drosophila* embryos after fertilization. For each RNA target, two kinds of OMUpy2s were used. Their fluorescence spectra were measured with a microspectroscope. They showed a typical bis-pyrene fluorescence spectra having a maximum around 480 nm. The relative expression levels between the six kinds of RNA targets were estimated from the fluorescence intensity at 480 nm (Figure 5c. (1)). There were a little differences in the fluorescence intensities of the two kinds of OMUpy2 for the same target RNA, respectively, but the tendency of the relative RNA expression levels in the six kinds of target RNA are similar between the two kinds of OMUpy2 for the same RNA. The average of the fluorescence intensities by the two kinds of OMUpy2 for the same target mRNA was shown in Figure 5c. (2). The relative expression levels of the six kinds of RNA targets were similar to the tendency of total amount of 0-10-hr RNA expression levels shown in the database (FlyBase) [41] (Figure 5c. (2) right). The expression level of eve was the lowest and the expression level of Kr was the highest in the six kinds of RNAs in both of database and experimental data. Relative values on the basis of the intensity of eve were shown above the bar graphs. The relative values of nos, gt, and ftz in experimental data were according to the relative values in database. These results indicate that it is possible to compare approximate relative RNA expression levels with OMUpy2.

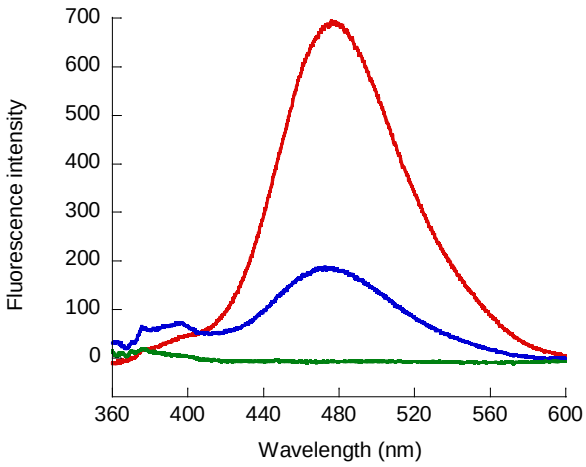

Figure 5a. Fluorescence spectra of Kr-OMUpy2 and Control-OMUpy2 in the presence or the absence of mRNA extracted from *Drosophila* embryos expressed Kr mRNA.

red line: Kr-OMUpy2/3-5-hr mRNA, blue line: Kr-OMUpy2/0-2-hr mRNA, green line: Control-OMUpy2/3-5-hr mRNA, [Kr-OMUpy2] = [Control-OMUpy2] = 30 μM [mRNA] = 65 mg/ml, 10 mM phosphate buffer (pH 7.0) containing 100 mM NaCl.

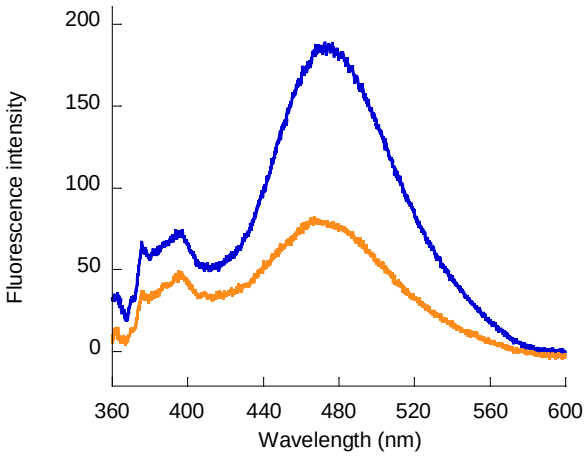

Figure 5b. Competition assay by Kr-OMUnonpy.

blue line: Kr-OMUpy2/0-2-hr mRNA, orange line: Kr-OMUnonpy/Kr-OMUpy2/ 0-2-hr mRNA, [Kr-OMUpy2] = 30 μM, [Kr-OMUnonpy] = 15 μM, [mRNA] = 65 mg/ml, 10 mM phosphate buffer (pH 7.0) containing 100 mM NaCl.

(1)

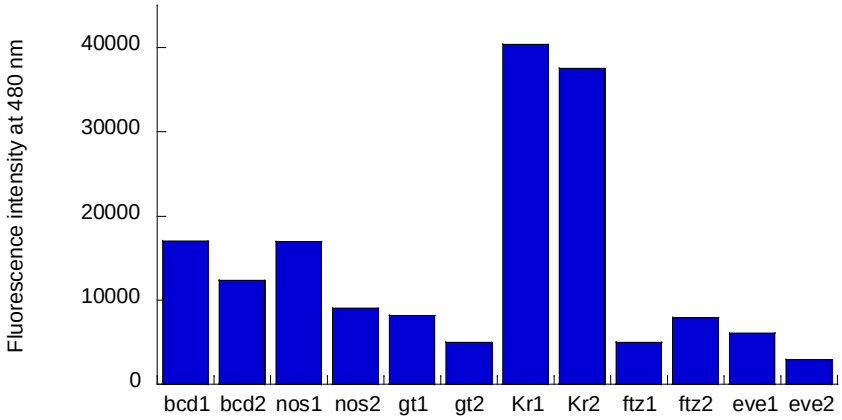

(2)

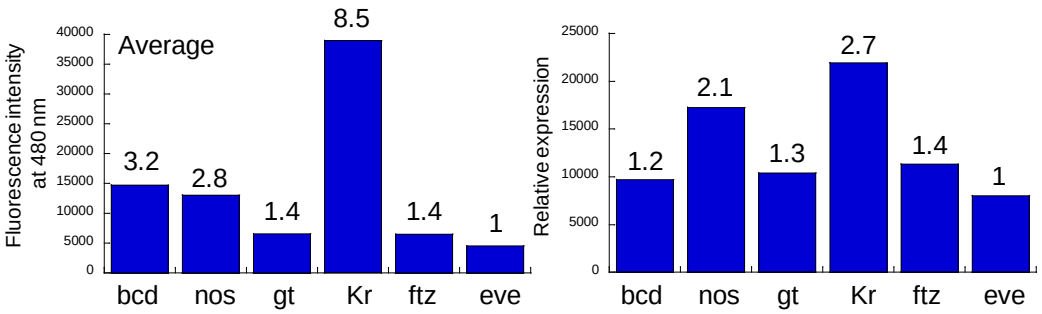

Figure 5c. Fluorescence intensity at 480 nm for the six types of RNA targets and relative RNA expression levels.

(1) [OMUpy2] = 8 μM, [total RNA] = 70 mg/ml, 10 mM phosphate buffer (pH 7.0) containing 100 mM NaCl, total RNA was extracted from 0-9hr embryos. (2) left: The average of fluorescence intensity of the two kinds of OMUpy2 for the same target mRNA. right: Relative RNA expression levels in 0-10hr embryos shown in the database (FlyBase: http://flybase.org/) The numbers above the bar graphs show a relative value on the basis of the intensity of eve.

1.3.5. The detection of target RNA in the fixed *Drosophila* embryo

The detection of Kr mRNA in the fixed embryos was carried out using both stage-1 and stage-5 embryos at the beginning of formation of the cellular blastoderm. Using a Kr-F whose 5' end was modified with fluorescein isothiocyannate (FITC), we first examined the distribution of probes in the fixed embryos at stage-5. Figure 6a.-A shows differential interference contrast (DIC) images of the embryo at the stage-5, and Figure 6a.-E shows the fluorescence image after careful washing of Kr-F with PBT once. The fluorescent signal of Kr-F was detected in the entire region of the embryo, indicating that probes were almost evenly distributed in the embryo.

Next OMUpy2 was applied to the detection of target RNA in fixed *Drosophila* embryos with just one washing step by PBT. Figures 6a.-B and-C show the DIC images of the embryos at stage-5 after treatment with Kr-OMUpy2 and Control-OMUpy2, respectively. Figure 6a.-D shows the result with an early embryo (stage-1) prior to nuclei migration toward the cortex. In the embryo at stage-1, Kr mRNA is not expressed yet. In stage-5 embryo treated with Kr-OMUpy2, a fluorescent signal was apparently detected in the center region and around the posterior region of the embryo (Figure 6a.-F, Figure 6c.-E-H.). The localization of the signal in the center region of the embryo corresponds to the reported Kr mRNA expression pattern in early embryos [9, 24-26]. The signal obtained in the posterior region of the embryo was similar to the observation reported by Hoch *et al*. [42]. In the case of stages-5 embryo treated with Control-OMUpy2, no fluorescence was observed (Figure 6a. G). Similarly, in the stages-1 embryo treated with Kr-OMUpy2, no fluorescence was observed (Figure 6a.-H). To confirm whether the signal in the stage-5 embryo treated with the Kr-OMUpy2 (Figure 6a.-F) was derived from the bis-pyrene moiety, the fluorescence spectra were measured with a microspectroscope (Figure 6b.). The spectrum of the stage-5 embryo treated with Kr-OMUpy2 peaked at around 480 nm (Figure 6a.-F and 6b), and it was a waveform similar to the fluorescence spectrum of the Kr-OMUpy2/Kr-ORN solution (Figure 3a.). In the spectrum of the stage-5 embryo untreated with probes, small fluorescence considered to be the autofluorescence of an embryo was observed. The fluorescence observed in the spectra of the stage-5 embryo

treated with Control-OMUpy2 and the stage-1 embryo treated with Kr-OMUpy2 were no significant difference compared with the autofluorescence of an embryo (Figure 6b.). These results also support that Kr-OMUpy2 detected Kr mRNA sequence specifically. The embryos treated with the other OMUpy2 probes for bcd, nos, gt, ftz, and eve were not observed fluorescence well. It is thought that this result relates to that Kr mRNA was the most amount of expression of the six kinds of RNA. The detection of target RNA by WISH is much more difficult than the detection of target RNA in the total RNA extract because the success of the detection of target RNA in the fixed embryo largely depends on the states of the specimen. It is not easy to solve this problem. But it is essential to improve various points including OMUpy2 for more successful detection RNA in *Drosophila* embryo.

OMUpy2 has improved the protocol of whole-mount *in situ* hybridization in the washing step. OMUpy2 enabled to the observation after a single wash because it does not emit unless bound to the target RNA. In the commonly used *in situ* RNA hybridization methods with *Drosophila* embryos, the steps from the embryo fixation to observation take at least 3 days [10, 29]. In that protocol, cDNA probes are prepared by reverse transcription reaction on mRNA, and their lengths are usually more than 100-nt. Using these cDNA probes, it can take a long time, sometimes one day, to attain optimum hybridization with the target mRNA in the fixed embryos. And the repeats of washing steps are inevitably necessary to remove unbound signals. In contrast, using Kr-OMUpy2, several washing steps could be omitted and the hybridization time was shortened to a few hours. This was attributed to the unique characteristics of Kr-OMUpy2 which consists of a short oligonucleotide (15-nt) and emits signals only when excited in the presence of its complementary RNA. Therefore, unbound Kr-OMUpy2 can be ignored in imaging protocols.

The development of RNA research has inaugurated a new era of life science, and the ripple effects extend to many different fields of life science. This study focuses on the technology aiming at RNA based diagnosis, which could be a key to research in the future life sciences including medical science. From the information obtained by DNA diagnosis, we can understand the presence of genetic alteration in specimens such

as cells, tissue, and organs. For example, the finding of a single base alteration in DNA suggests the possibility that the cells may develop into cancerous cells. However, this alteration does not always mean the onset of cancer. In medical diagnosis, it is quite important to find the signs of transformation in cells prior to their development into malignancy. RNA could be a suitable target for detecting signs of cancerous change in cells [5, 6]. In this study, we demonstrated that RNA specific probe, OMUpy2, was applicable to the estimation of relative RNA expression level in the total RNA extract. We also showed the possibility of OMUpy2 as a probe to detect RNA target in *Drosophila* embryo with relatively quick and easy protocol. The promising results of this manuscript show the great potential of RNA-based detection for both biological research and diagnostic medicine.

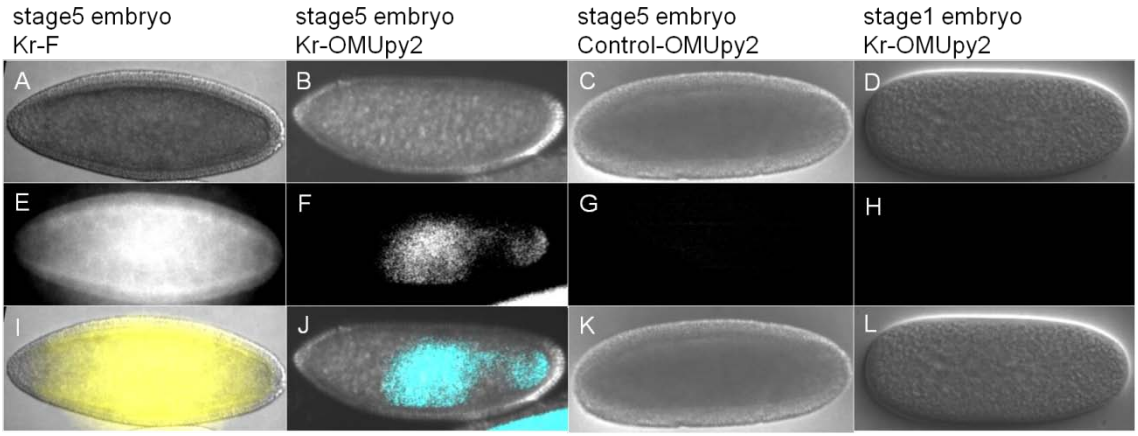

Figure 6a. Differential Interference Contrast (DIC) and fluorescent images of fixed *Drosophila* embryos.

Anterior is to the left. (A-D) DIC (differential interference contrast) images. (E-H) Fluorescence images. (I-L) merge images. [OMUpy2] = [Kr-F] = 30 μM, OMUpy2: (Ex: 340/15 nm, Em: 480/30 nm), Kr-F: (Ex: 470/20 nm, Em: 520 nm (BA)) Objective: Plan Fluor 20x, NA: 0.45, The merge images were converted to pseudo-color (I, yellow; J, blue)

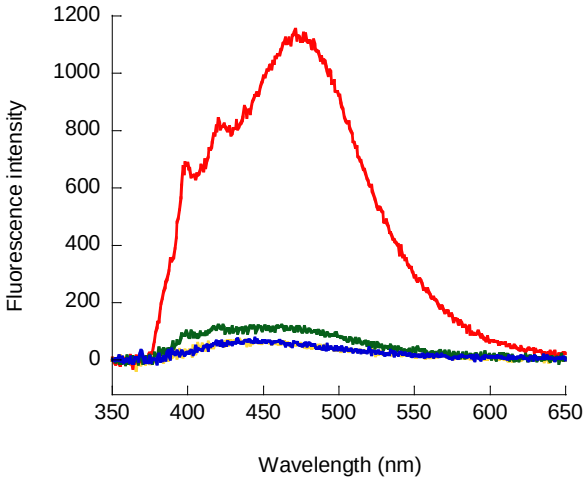

Figure 6b. Microscopic fluorescence spectra of the embryos after whole-mount *in situ* hybridization.

red line: stage-5 embryo treated with Kr-OMUpy2, green line: stage-5 embryo treated with Control-OMUpy2, blue line: stage-5 embryo untreated with probes, yellow line: stage-1 embryo treated with Kr-OMUpy2. Ex: 340/15 nm, DM: 380 nm, exposure time: 5 s.

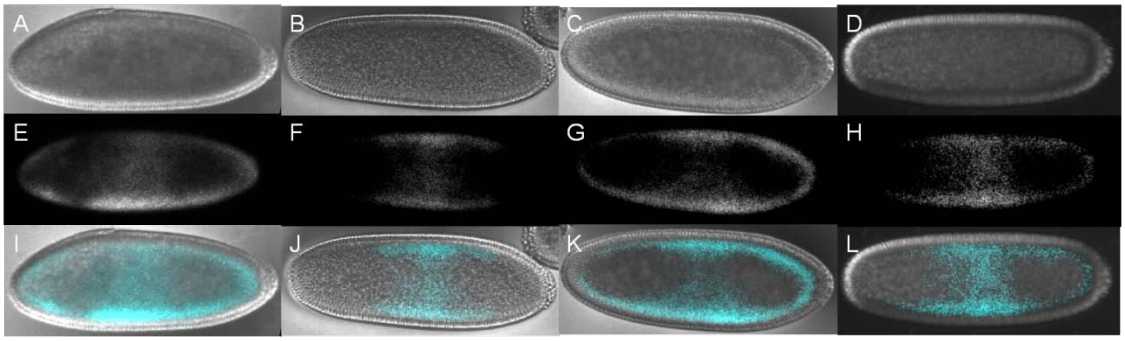

Figure 6c. Differential Interference Contrast (DIC) and fluorescent images of fixed *Drosophila* embryos treated with Kr-OMUpy2.

Anterior is to the left. (A-D) DIC (differential interference contrast) images. (E-H) Fluorescence images. (I-L) merge images. [OMUpy2] = 30 μM, OMUpy2: (Ex: 340/15 nm, Em: 480/30 nm), Objective: Plan Fluor 20x, NA: 0.45, The merge images were converted to pseudo-color (blue).

References

1. Tang, G. (2005) siRNA and miRNA: an insight into RISCs. *Trends Biochem. Sci.*, 30, 2, 106-114.
2. Pall, G.S., Hamilton, A.J. (2008) Improved northern blot method for enhanced detection of small RNA. *Nat. Protoc.*, 3, 6, 1077-1084.
3. Gibson, U.E., Heid, C.A., Williams, P.M. (1996) A novel method for real time quantitative RT-PCR. *Genome Res.*, 6, 10, 995-1001.
4. Schena, M., Shalon, D., Davis, R.W., Brown, P.O. (1995) Quantitative monitoring of gene expression patterns with a complementary DNA microarray. *Science*, 270, 5235, 467-470.
5. Sunde, R.A. (2010) mRNA transcripts as molecular biomarkers in medicine and nutrition. *J. Nutr. Biochem.*, 21, 665-670.
6. Zhang, Q., Pu, R., Du, Y., Han, Y., Su, T., Wang, H., Cao, G. (2012) Non-coding RNAs in hepatitis B or C-associated hepatocellular carcinoma: potential diagnostic and prognostic markers and therapeutic targets. *Cancer Lett.*, 321, 1-12.
7. Chan, K.H., Poon, L.L., Cheng, V.C., Guan, Y., Hung, I.F., Kong, J., Yam, L.Y., Seto, W.H., Yuen, K.Y., Peiris, J.S. (2004) Detection of SARS coronavirus in patients with suspected SARS. *Emerg. Infect. Dis.*, 10, 294-299.
8. Delamare, C., Burgard, M., Mayaux, M.J., Blanche, S., Doussin, A., Ivanoff, S., Chaix, M.L., Khan, C., Rouzioux, C. (1997) HIV-1 RNA detection in plasma for the diagnosis of infection in neonates. The French Pediatric HIV Infection Study Group. *J. Acquir. Immune. Defic. Syndr. Hum. Retrovirol.*, 15, 121-125.
9. Tautz, D., Pfeifle, C. (1989) A non-radioactive in situ hybridization method for the localization of specific RNAs in *Drosophila* embryos reveals translational control of the segmentation gene hunchback. *Chromosoma*, 98, 2, 81-85.
10. Weiszmann, R., Hammonds, A.S., Celniker, S.E. (2009) Determination of gene expression patterns using high-throughput RNA in situ hybridization to whole-mount *Drosophila* embryos. *Nat. Protoc.*, 4, 605-618.
11. Lécuyer, E., Parthasarathy, N., Krause, H.M. (2008) Fluorescent in situ hybridization protocols in *Drosophila* embryos and tissues. *Methods Mol. Biol.*, 420, 289-302.
12. Kosman, D., Mizutani, C.M., Lemons, D., Cox, W.G., McGinnis, W., Bier, E. (2004) Multiplex detection of RNA expression in *Drosophila* embryos. *Science.* 305, 846.
13. Okamoto, A., Tanabe, K., Inasaki, T., Saito, I. (2003) Phototriggered drug release from functionalized oligonucleotides by a molecular beacon strategy. *Angew. Chem. Int. Ed. Engl.*, 42, 2502-2504.
14. Bao, G., Rhee, W.J., Tsourkas, A. (2009) Fluorescent probes for live-cell RNA detection. *Annu. Rev. Biomed. Eng.*, 11, 25-47.
15. Santangelo, P.J., Nix, B., Tsourkas, A., Bao, G. (2004) Dual FRET molecular

beacons for mRNA detection in living cells. *Nucleic Acids Res*., 32, e57.

16. Abe, H., Kool, E.T. (2006) Flow cytometric detection of specific RNAs in native human cells with quenched autoligating FRET probes. *Proc. Natl. Acad. Sci. U. S. A.*, 103, 263-268.
17. Kurokawa, K., Mochizuki, N., Ohba, Y., Mizuno, H., Miyawaki, A., Matsuda, M. (2001) A pair of fluorescent resonance energy transfer-based probes for tyrosine phosphorylation of the CrkII adaptor protein in vivo. *J. Biol. Chem.*, 276, 31305-31310.
18. Mahara, A., Iwase, R., Sakamoto, T., Yamana, K., Yamaoka, T., Murakami, A. (2002) Bispyrene-conjugated 2'-*O*-methyloligonucleotide as a highly specific RNA-recognition probe. *Angew. Chem. Int. Ed. Engl*., 41, 19, 3648-3650.
19. Maie, K., Nakamura, M., Takada, T., Yamana, K. (2009) Fluorescence quenching properties of multiple pyrene-modified RNAs. *Bioorg. Med. Chem.*, 17, 14, 4996-5000.
20. Mahara, A., Iwase, R., Sakamoto, T., Yamaoka, T., Yamana, K., Murakami, A. (2003) Detection of acceptor sites for antisense oligonucleotides on native folded RNA by fluorescence spectroscopy. *Bioorg. Med. Chem.*, 11, 13, 2783-2790.
21. Nakamura, M., Fukunaga, Y., Sasa, K., Ohtoshi, Y., Kanaori, K., Hayashi, H., Nakano, H., Yamana, K. (2005) Pyrene is highly emissive when attached to the RNA duplex but not to the DNA duplex: the structural basis of this difference. *Nucleic Acids Res.*, 33, 18, 5887-5895.
22. Nüsslein-Volhard, C., Wieschaus, E. (1980) Mutations affecting segment number and polarity in *Drosophila*. Nature, 287, 5785, 795-801.
23. Knipple, D.C., Seifert, E., Rosenberg, U.B., Preiss, A., Jäckle, H. (1985) Spatial and temporal patterns of Krüppel gene expression in early *Drosophila* embryos. *Nature*, 317, 6032, 40-44.
24. Tsai, C., Gergen, J.P. (1994) Gap gene properties of the pair-rule gene runt during *Drosophila* segmentation. *Development*, 120, 6, 1671-1683.
25. Schulz, C., Tautz, D. (1994) Autonomous concentration-dependent activation and repression of Krüppel by hunchback in the *Drosophila* embryo. *Development*, 120, 10, 3043-3049.
26. Jaeger, J., Sharp, D.H., Reinitz, J. (2007) Known maternal gradients are not sufficient for the establishment of gap domains in *Drosophila melanogaster. Mech. Dev*., 124, 2, 108-128.
27. Surkova, S., Kosman, D., Kozlov, K., Manu, Myasnikova, E., Samsonova, A.A., Spirov, A., Vanario-Alonso, C.E., Samsonova, M., Reinitz, J. (2008) Characterization of the *Drosophila* segment determination morphome. *Dev. Biol.*, 313, 2, 844-862.
28. Wincott, F., DiRenzo, A., Shaffer, C., Grimm, S., Tracz, D., Workman, C., Sweedler, D., Gonzalez, C., Scaringe, S., Usman, N. (1995) Synthesis, deprotection, analysis and purification of RNA and ribozymes. *Nucleic Acids Res.*, 23, 14, 2677-2684.

29. Hughes, S.C., Krause, H.M. (1999) Single and double FISH protocols for *Drosophila*. *Methods Mol. Biol*., 122, 93-101.
30. Mathews, D.H., Sabina, J., Zuker, M., Turner, D.H. (1999) Expanded Sequence Dependence of Thermodynamic Parameters Improves Prediction of RNA Secondary Structure. *J. Mol. Biol.*, 288, 911-940.
31. http://rna.urmc.rochester.edu/RNAstructure.html
32. Xia, T., SantaLucia, J.Jr., Burkard, M.E., Kierzek, R., Schroeder, S.J., Jiao, X., Cox, C., Turne,r D.H. (1998) Thermodynamic parameters for an expanded nearest-neighbor model for formation of RNA duplexes with Watson-Crick pairs. *Biochemistry*, 37, 14719–14735.
33. Mathews, D.H., Disney, M.D., Childs, J.L., Schroeder, S.J., Zuker, M., Turner, D.H. (2004) Incorporating chemical modification constraints into a dynamic programming algorithm for prediction of RNA secondary structure. *Proc. Natl. Acad. Sci. U.S.A.*, 101, 7287–7292.
34. Yamayoshi, A. Photodynamic antisense regulation of human cervical carcinoma cell growth using psoralen-conjugated oligonucleotides. Kyoto, Japan: Kyoto Institute of Technology; 2003, Thesis.
35. Molenaar, C., Marras, S.A., Slats, J.C., Truffert, J.C., Lemaître, M., Raap, A.K., Dirks, R.W., Tanke, H.J. (2001) Linear 2' *O*-Methyl RNA probes for the visualization of RNA in living cells. *Nucleic Acids Res*., 29, 17, E89-9.
36. Sixou, S., Szoka, F.C. Jr, Green, G.A., Giusti, B., Zon, G., Chin, D.J. (1994) Intracellular oligonucleotide hybridization detected by fluorescence resonance energy transfer (FRET). *Nucleic Acids Res*., 22, 4, 662–668.
37. Czauderna, F., Fechtner, M., Dames, S., Aygün, H., Klippel, A., Pronk, G.J., Giese, K., Kaufmann, J. (2003) Structural variations and stabilising modifications of synthetic siRNAs in mammalian cells. *Nucleic Acids Res*., 31, 11, 2705-2716.
38. Kubota, T., Ikeda, S., Yanagisawa, H., Yuki, M., Okamoto, A. (2009) Hybridization-sensitive fluorescent probe for long-term monitoring of intracellular RNA. *Bioconjug. Chem*., 20, 6, 1256-1261.
39. Tsourkas, A., Behlke, M.A., Bao, G. (2003) Hybridization of 2'-*O*-methyl and 2'-deoxy molecular beacons to RNA and DNA targets. *Nucleic Acids Res.*, 31, 6, 5168-5174.
40. Bratu, D.P., Cha, B.J., Mhlanga, M.M., Kramer, F.R., Tyagi, S. (2003) Visualizing the distribution and transport of mRNAs in living cells. *Proc. Natl. Acad. Sci. U.S.A.*, 100, 23, 13308-13313.
41. FlyBase: http://flybase.org/
42. Hoch, M., Schröder, C., Seifert, E., Jäckle, H. (1990) cis-acting control elements for Krüppel expression in the *Drosophila* embryo. *EMBO J.*, 9, 2587-2595.

Chapter 2

The quantitative analysis of RNA expression with RNA specific probes

2.1 Introduction

Many kinds of miRNAs have been found out one after another since the first discovery in 1983 [1-4]. It has been revealed that miRNA is a molecule which suppresses post-transcriptional level of mRNA translation in general [5-7]. Especially, miRNA is involved in development and homeostasis, which means that the collapse of miRNA regulation leads to various diseases. In recent years, it has been revealed that the aberrant expression of miRNA is related to diseases such as cancer [2, 3, 8-10], cardiac disease [11, 12], rheumatism [13], and Alzheimer disease [14, 15]. miRNA can be used as biomarkers of diagnosis, progression, and prognosis because many of miRNAs involved in certain diseases show characteristic expressions [16]. Though the expressions of many miRNAs related to the diseases have been investigated by microarray, probing, PCR assay, and northern blotting, most of them were the evaluation of relative expression levels or the existences of miRNAs [17-19]. In most of other RNAs as well as miRNAs, average molecular copy number per cell is not estimated though the relative expression levels are investigated. Therefore to calculate the average molecule number of expressed RNA in a cell is a significant challenge even if it is evaluated approximately.

With the aim of RNA diagnosis which can evaluate expression level in total RNA extracts, we examined the abundance of target RNA in total RNA extracted from HeLa cells using RNA specific probe, OMUpy2. Two characteristics of OMUpy2 make it possible to decide the expression level of target RNA in the total RNA extract with the relations between fluorescence intensity and RNA concentration shown from OMUpy2 and its complementary RNA solution. The first is that OMUpy2 binds to target RNA in a one-to-one emission. Second is that OMUpy2 emits fluorescence at around 480 nm

only when it bound to target RNA [20, 21].

2.2 Materials and Methods

2.2.1. Cell line

Human cervical carcinoma cell line, HeLa, was grown in Dulbecco's modified Eagle's Medium (DMEM) supplemented with 10 % fetal bovine serum, 25 units/mL penicillin and 25 mg/mL streptomycin at 37 °C in a humidified chamber with 5 % CO_2.

2.2.2. Extraction of total RNA from HeLa cells

Total RNA was extracted from 1×10^7 HeLa cells with 4 mL of TRIzol® Reagent (Invitrogen). After stirring, 800 μL chloroform/isoamyl alcohol (49/1, v/v) were added, and followed by vigorous shaking. After incubation on ice for 5 min, the suspension was centrifuged at 10,000 rpm at 4 °C for 15 min. RNA in the aqueous phase was transferred to a sterilized tube. After addition of 2 mL of isopropanol to the tube, the solution was stored on ice for 5 min followed by centrifugation at 10,000 rpm at 4 °C for 10 min. Isopropanol was exchanged with 75 % aq. ethanol and the ethanol solution was centrifuged at 7,500 rpm at 4 °C for 3 min three times. Decant the supernatant, removing as much as possible without disturbing the pellet. Air-dry RNA pellet.

2.2.3. Fluorescence measurements of OMUpy2 hybridized with complementary oligo RNA (ORN) and OMUpy2 hybridized with target RNA in total RNA extract

Fluorescence measurements of OMUpy2 hybridized with complementary oligo RNA (ORN) and OMUpy2 hybridized with total RNA extracted from *Drosophila* embryos were measured with a spectrofluorophotometer (RF-5300PC, Shimadzu). The concentration of ORN on creating calibration plots was changed in the range of 10 nM to 1000 nM. The concentration of total RNA used for measurements was 1400 μg/mL and that of OMUpy2s were each 1 μM in 10 mM phosphate buffer containing 100 mM NaCl (pH 7.0). The excitation wavelength of fluorophore (OMUpy2) was 342 nm.

2.3 Results and Discussion

2.3.1. Probe preparation

As target RNAs, 28S rRNA, hsa-mir-21, hsa-mir-24-2, hsa-mir-29a, and U6 snRNA were chosen. miR-21 is one of the most commonly and highly upregulated miRNA in many kinds of cancer [22, 23]. miR-21, miR-24, and miR-29 are highly transcribed in a HeLa cell [24]. The relative expression levels of them are high in order of miR-21, miR-24, and miR-29 [24]. The expression level of U6 sn RNA is also high in a HeLa cell [25].

OMUpy2 were synthesized according to previous reports and purified by reverse phase HPLC [21]. The details of the sequences were shown in Table 1. The fluorescence spectra of duplex between OMUpy2 and their ORN solution were peaked at around 480 nm.

Table 1. Sequences used in the present study.

target RNA	name	5' SEQUENCES 3' upper: target RNA / lower: probe	Nucleotide positions	GenBank ID/ miRBase Accession
28S rRNA	28S-ORN	CGC UCA UCA GAC CCC AGA AAA G	1903-1924	337381
	28S-OMUpy2	*CUU UUC UGG GG*Upy Cpy*UG AUG AGC G*		
hsa-mir-21	miR21-ORN	UAG CUU AUC AGA CUG AUG UUG A	8-29	MI0000077
	miR21-OMUpy2	*UCA ACA UCA G*UpyCpy *UGA UAA GCU A*		
hsa-mir-24-2	miR24-ORN	UGG CUC AGU UCA GCA GGA ACA G	50-71	MI0000081
	miR24-OMUpy2	*CUG UU*Cpy Cpy*UG CUG AAC UGA GCC A*		
hsa-mir-29a	miR29-ORN	UAG CAC CAU CUG AAA UCG GUU A	42-63	MI0000087
	miR29-OMUpy2	*UAA CCG AUpyUpy UCA GAU GGU GCU A*		
U6 snRNA	U6 snRNA	ACG CAA AUU CGU GAA GCG UU	16-36	174943
	U6-OMUpy2	*AAC GCU UCA CGA AUpyUpy UGC GU*		

Italic letters: 2'-OMe nucleotides, capital letters: ribonucleotides.

2.3.2. The calibration plots of the fluorescence intensity at 480 nm corresponding to ORN concentration

In order to create the calibration plots of the fluorescence intensity at 480 nm corresponding to ORN concentration, the fluorescence intensity at 480 nm of OMUpy2 in the presence of the complementary ORN (cORN) was measured in the range of 10 nM to 1000 nM cORN concentration. The fluorescence intensity of OMUpy2-cORN hybrids versus the concentration of cORN had a linear relationship as shown in Figure 1.

(1)

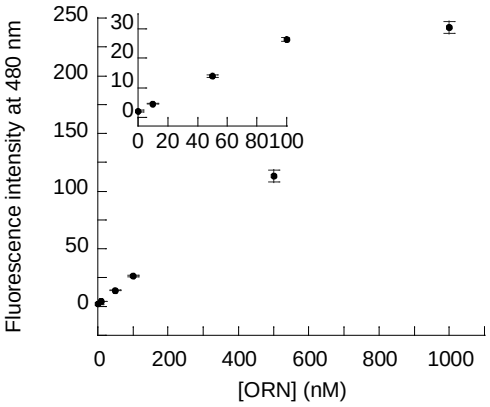

(2)

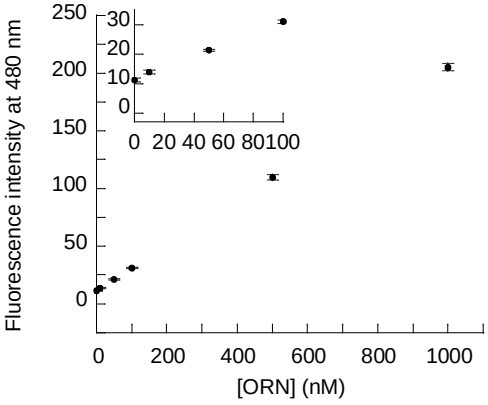

(3)

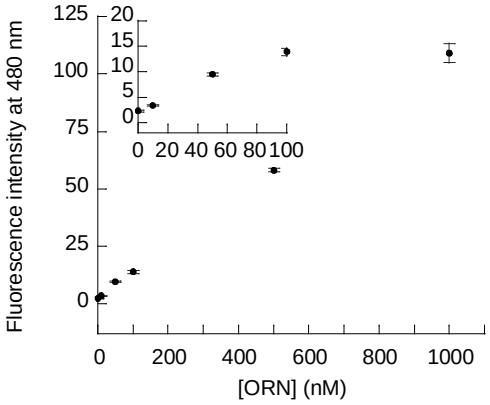

(4)

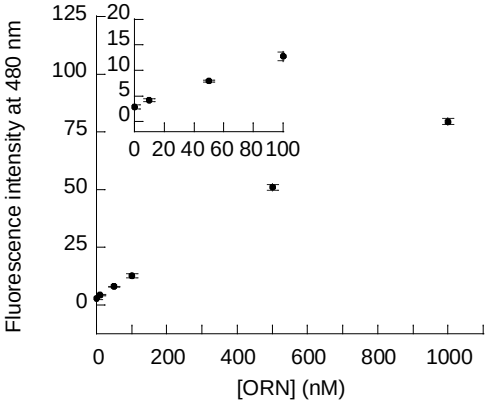

(5)

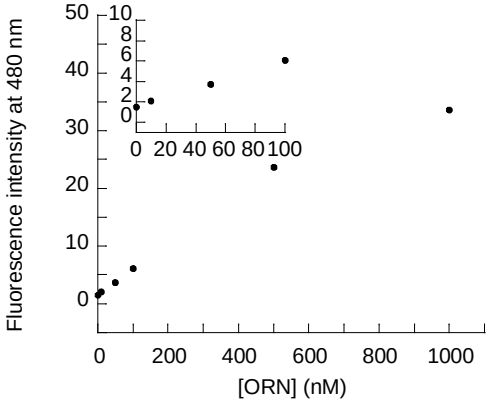

Figure 1. The calibration plots of the fluorescence intensity at 480 nm corresponding to ORN concentration

(1) 28S-OMUpy2/ORN,
(2) miR21-OMUpy2/ORN,
(3) miR24-OMUpy2/ORN,
(4) miR29-OMUpy2/ ORN,
(5) U6-OMUpy2/ORN,
[28S-OMUpy2] = [miR21-OMUpy2] = [miR24-OMUpy2] = [miR29-OMUpy2] = [U6-OMUpy2] = 1000 nM, [ORN] = 10 nM-1000 nM in 10 mM phosphate buffer (pH 7.0) containing 100 mM NaCl, 20 °C, λex=342 nm, λem = 480 nm.

2.3.3. The quantitative analysis of RNA expression levels in a HeLa cell caluculated from fluorescence intensity of OMUpy2

To quantify the amount of RNA expression in a cell, the fluorescence spectra of OMUpy2 and total RNA solution extracted from 1×10^7 HeLa cells were measured (Figure 2.). To determine the molecular abundance of target RNA in a cell, the fluorescence signals of the hybridization between OMUpy2 and target RNA in the total RNA were compared with the calibration plots (Figure 3.). The number of mir-21, 10^4 molecules per cell, corresponded to a previous report by Lee *et al*. [26]. The number of U6 snRNA was one order of magnitude smaller than previously reported by Lee *et al*. [26]. Though the relative expression of miR-29 compared to miR-21 is reported to be about one tenth by Schmittgen *et al*. [17], our result was larger than that. miRNAs are transcribed as long primary transcripts (pri-miRNAs) whose maturation occurs through following processing; the nuclear processing of the pri-miRNAs into stem-loop precursors, 70 nucleotides (pre-miRNAs), and the cytoplasmic processing of pre-miRNAs into mature miRNAs [27]. OMUpy2 cannot distinguish that the detected miRNAs are at any of these stages. But it is a great advantage to be able to detect target RNA without the amplification of total RNA extract because an error based on the amplification efficiency does not occur. In order to adequately characterize the expression of miRNA, it may be necessary to quantify both of mature and precursor miRNA. Inferring the exact RNA expression level is difficult, but even approximation of RNA expression level would give us useful information to assist the judgment of diagnosis, progress, and prognosis of various diseases.

(1)

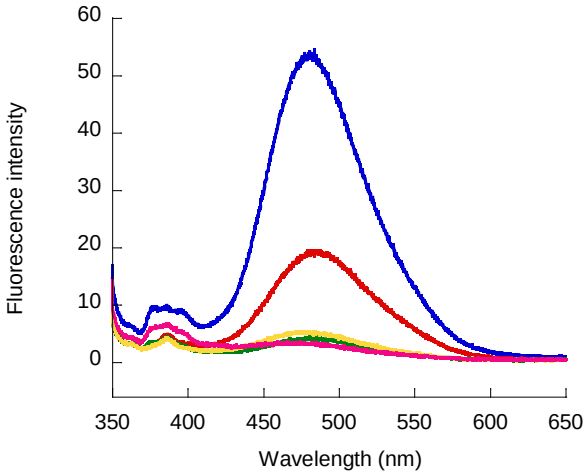

(2)

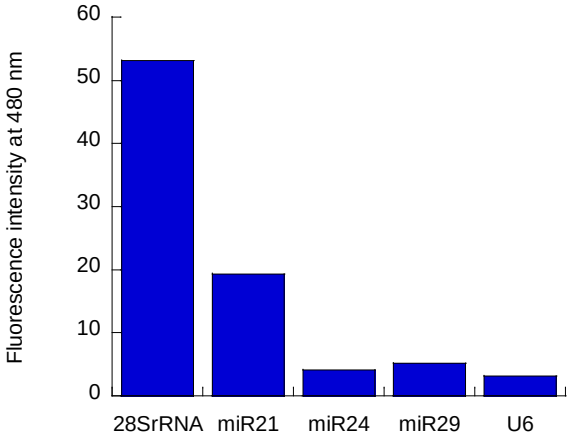

Figure 2. (1) Fluorescence spectra of OMUpy2 in the presence of total RNA. (2) Fluorescence intensity at 480 nm.

blue line: 28S-OMUpy2/total RNA, red line: miR21-OMUpy2/total RNA, green line: miR24-OMUpy2/total RNA, yellow line: miR29-OMUpy2/total RNA, pink line: U6-OMUpy2/total RNA, Conditions: [28S-OMUpy2] = [miR21-OMUpy2] = [miR24-OMUpy2] = [miR29-OMUpy2] = [U6-OMUpy2] = 1 μM, [total RNA] = 1400 μg/mL in 10 mM phosphate buffer (pH 7.0) containing 100 mM NaCl, 20 °C, λex = 342 nm.

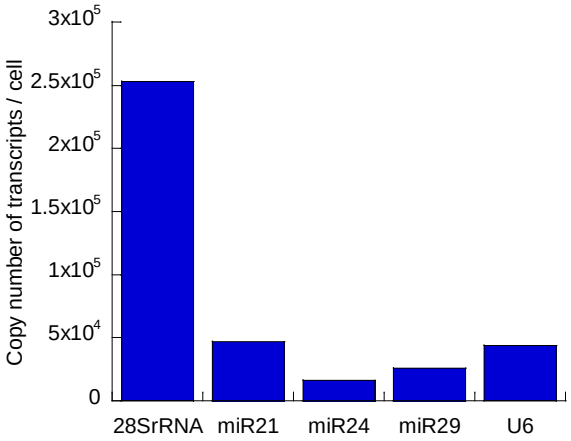

Figure 3. The quantitative analysis of RNA expression in a cell.

Molecular abundance of 28S rRNA, miRNAs, and U6 snRNA. Copy numbers of the transcript per cell were calculated from fluorescence intensity (Figure1. and Figure 2.).

References

1. Lee, R.C., Feinbaum, R.L., Ambros, V. (1993) The *C. elegans* heterochronic gene lin-4 encodes small RNAs with antisense complementarity to lin-14. *Cell*, 75, 843-854.
2. Tekotte, H., Davis, I. (2002) Intracellular mRNA localization: motors move messages. *Trends Genet*., 18, 636-642.
3. Iorio, M.V., Ferracin, M., Liu, C.G., Veronese, A., Spizzo, R., Sabbioni, S., Magri, E., Pedriali, M., Fabbri, M., Campiglio, M., Ménard, S., Palazzo, J.P., Rosenberg, A., Musiani, P., Volinia, S., Nenci, I., Calin, G.A., Querzoli, P., Negrini, M., Croce, C.M. (2005) MicroRNA gene expression deregulation in human breast cancer. *Cancer Res*., 65, 7065-7070.
4. Johnson, S.M., Grosshans, H., Shingara, J., Byrom, M., Jarvis, R., Cheng, A., Labourier, E., Reinert, K.L., Brown, D., Slack, F.J. (2005) RAS is regulated by the let-7 microRNA family. *Cell*., 120, 635-647.
5. Kim, V.N. (2005) MicroRNA biogenesis: coordinated cropping and dicing. *Nat Rev Mol Cell Biol*., 6, 376-385.
6. Bartel, D.P. (2004) MicroRNAs: genomics, biogenesis, mechanism, and function. *Cell*., 116, 281-297.
7. Bushati, N., Cohen, S.M. (2007) microRNA functions. *Annu. Rev. Cell Dev. Biol*., 3, 175-205.
8. Yanaihara, N., Caplen, N., Bowman, E., Seike, M., Kumamoto, K., Yi, M., Stephens, R.M., Okamoto, A., Yokota, J., Tanaka, T., Calin, G.A., Liu, C.G., Croce, C.M., Harris, C.C. (2006) Unique microRNA molecular profiles in lung cancer diagnosis and prognosis. *Cancer Cell*., 9, 189-198.
9. Volinia, S., Calin, G.A., Liu, C.G., Ambs, S., Cimmino, A., Petrocca, F., Visone, R., Iorio, M., Roldo, C., Ferracin, M., Prueitt, R.L., Yanaihara, N., Lanza, G., Scarpa, A., Vecchione, A., Negrini, M., Harris, C.C., Croce, C.M. (2006) A microRNA expression signature of human solid tumors defines cancer gene targets. *Proc. Natl. Acad. Sci. U. S. A*., 103, 2257-2261.
10. Calin, G.A., Croce, C.M. (2006) MicroRNA signatures in human cancers. *Nat. Rev. Cancer*., 6, 857-866.
11. Carè, A., Catalucci, D., Felicetti, F., Bonci, D., Addario, A., Gallo, P., Bang, M.L., Segnalini, P., Gu, Y., Dalton, N.D., Elia, L., Latronico, M.V., Høydal, M., Autore, C., Russo, M.A., Dorn, G.W., Ellingsen, O., Ruiz-Lozano, P., Peterson, K.L., Croce, C.M., Peschle, C., Condorelli, G. (2007) MicroRNA-133 controls cardiac hypertrophy. *Nat. Med.*, 13, 613-618.
12. van Rooij, E., Marshal,l W.S., Olson, E.N. (2008) Toward microRNA-based therapeutics for heart disease: the sense in antisense. *Circ. Res*., 103, 919-928.
13. Nakasa, T., Miyaki, S., Okubo, A., Hashimoto, M., Nishida, K., Ochi, M., Asahara, H. (2008) Expression of microRNA-146 in rheumatoid arthritis synovial tissue. *Arthritis Rheum*., 58, 1284-1292.

14. Hébert, S.S., Horré, K., Nicolaï, L., Papadopoulou, A.S., Mandemakers, W., Silahtaroglu, A.N., Kauppinen, S., Delacourte, A., De Strooper, B. (2008) Loss of microRNA cluster miR-29a/b-1 in sporadic Alzheimer's disease correlates with increased BACE1/beta-secretase expression. *Proc. Natl. Acad. Sci. U. S. A.*, 105, 6415-6420.
15. Wang, W.X., Rajeev, B.W., Stromberg, A.J., Ren, N., Tang, G., Huang, Q., Rigoutsos, I., Nelson, P.T. (2008) The expression of microRNA miR-107 decreases early in Alzheimer's disease and may accelerate disease progression through regulation of beta-site amyloid precursor protein-cleaving enzyme 1. *J. Neurosci*., 28, 1213-1223.
16. Tricoli, J.V., Jacobson, J.W. (2007) MicroRNA: Potential for Cancer Detection, Diagnosis, and Prognosis. *Cancer Res.*, 67, 4553-4555.
17. Schmittgen, T.D., Jiang, J., Liu, Q., Yang, L. (2004) A high-throughput method to monitor the expression of microRNA precursors. *Nucleic Acids Res.*, 32, e43.
18. Gaur, A., Jewell, D.A., Liang, Y., Ridzon, D,, Moore, J.H., Chen, C., Ambros, V.R., Israel, M.A. (2007) Characterization of microRNA expression levels and their biological correlates in human cancer cell lines. *Cancer Res*., 67, 2456-2468.
19. Si, M.L., Zhu, S., Wu, H., Lu, Z., Wu, F., Mo, Y.Y. (2007) miR-21-mediated tumor growth. *Oncogene*. 26, 2799-2803.
20. Ueda, T., Kobori, A., Yamayoshi, A., Yoshida, H., Yamaguchi, M., Murakami, A. (2012) RNA-based diagnosis in a multicellular specimen by whole mount *in situ* hybridization using an RNA-specific probe. *Bioorg. Med. Chem*., 20, 6034-6039.
21. Mahara, A., Iwase, R., Sakamoto, T., Yamana, K., Yamaoka, T., Murakami, A. (2002) Bispyrene-conjugated 2'-*O*-methyloligonucleotide as a highly specific RNA-recognition probe. *Angew. Chem. Int. Ed. Engl*., 41, 19, 3648-3650.
22. Sayed, D., Rane, S., Lypowy, J., He, M., Chen, I.Y., Vashistha, H., Yan, L., Malhotra, A., Vatner, D., Abdellatif, M. (2008) MicroRNA-21 targets Sprouty2 and promotes cellular outgrowths. *Mol. Biol. Cell.*, 19, 8, 3272-3282.
23. Volinia, S., Calin, G.A., Liu, C.G., Ambs, S., Cimmino, A., Petrocca, F., Visone, R., Iorio, M., Roldo, C., Ferracin, M., Prueitt, R.L., Yanaihara, N., Lanza, G., Scarpa, A., Vecchione, A., Negrini, M., Harris, C.C., Croce, C.M. (2006) A microRNA expression signature of human solid tumors defines cancer gene targets. *Proc. Natl. Acad. Sci. U. S. A.*, 103, 7, 2257-2261.
24. Lau, N.C., Lim, L.P., Weinstein, E.G., Bartel, D.P. (2001) An abundant class of tiny RNAs with probable regulatory roles in Caenorhabditis elegans. *Science*, 294, 5543, 858-862.
25. Maroney, P.A., Chamnongpol, S., Souret, F., Nilsen, T.W. (2007) A rapid, quantitative assay for direct detection of microRNAs and other small RNAs using splinted ligation. *RNA*, 13, 6, 930-936.
26. Lim, L.P., Lau, N.C., Weinstein, E.G., Abdelhakim, A., Yekta, S., Rhoades,

M.W., Burge, C.B., Bartel, D.P. (2003) The microRNAs of Caenorhabditis elegans. *Genes. Dev*., 17, 991-1008.

27. Lee, Y., Jeon, K., Lee, J.T., Kim, S., Kim, V.N. (2002) MicroRNA maturation: stepwise processing and subcellular localization. *EMBO J*., 21, 4663-4670.

Chapter 3

The development of multi-colored FRET RNA probes

3.1 Introduction

Fluorescent microscopy techniques with dye-conjugated biomolecules have been used to elucidate the expressions, localizations, and movements of RNA [1, 2]. The multi-colored fluorescent probes enabled to simultaneously detect multiple RNA targets [3], transcription sites [4] and chromosomes [5] and have been applied to determine the spatial organization of two or even more types of biomolecules [6, 7]. Multiple separate images are taken with different excitation emission filter sets according to the fluorescent dyes. Therefore it is very difficult to monitor the expression of multiple RNA targets that are occuring at the same time using multi-excitation wavelength systems.

Kool [8, 9] reported excimer- and exciplex-based multicolor imaging systems. They synthesized oligodeoxyfluorosides with pyrene, benzopyrene, perylene, and stilbene derivatives at the 1’-position of nucleosides and took multicolor images with a single-excitation wavelength. Tong [10, 11] and Ohya [12] also reported combinatorial Förster resonance energy transfer (FRET) systems that exhibited different fluorescent emission patterns with a single-excitation wavelength and those were used in the multiplex detection of single nucleotide polymorphisms (SNPs). Based on these reports, multi-color fluorescent probes with a single-excitation wavelength are highly useful for biological assays and the development of new fluorescent probes having multi-color fluorescent dyes with a single-excitation wavelength is a challenging task.

To simultaneously visualize multiple RNA targets in a cell, it is necessary to develop probes which emit fluorescence with different colors when excited at a single-wavelength. Here we synthesized OMUpy2 with a cyanine dye conjugated at their 5’ end respectively. Cyanine dyes, Cy3 and Cy5, emit fluorescence around 570 nm or 670 nm when excited at 550 nm or 650 nm respectively (Figure 1.). Cy3 and Cy5

emit no fluorescence by the 342 nm excitation which is the excitation wavelength of pyrene. Cyanine dyes conjugated probes, Cy3-OMUpy2 and Cy5-OMUpy2, caused large Stokes shifts by FRET in the presence of the complementary RNA when excited at 342 nm. OMUpy2, Cy3-OMUpy2, and Cy5-OMUpy2 emitted blue, yellow and pink fluorescence respectively with single-wavelength excitation. It means that three RNA targets can be detected in a cell at the same time.

(1)

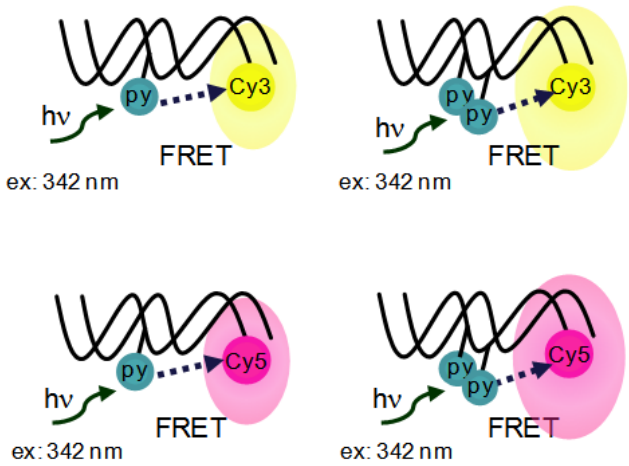

(2)

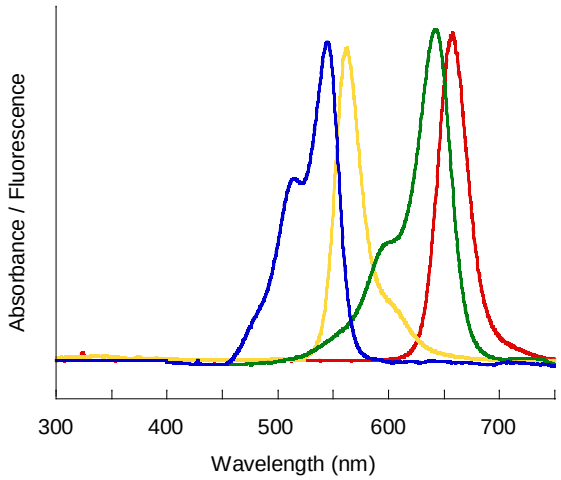

Figure 1. (1) Scheme of OMUpy and OMUpy2 modified with Cy3 or Cy5. (2) Absorption and fluorescence spectra of Cy3 and Cy5.

blue line: absorption spectrum of Cy3, yellow line: fluorescence spectrum of Cy3, green line: absorption spectrum of Cy5, red line: fluorescence spectrum of Cy5.

3.2 Materials and Methods

3.2.1. Probe preparation

Single-stranded region in the secondary RNA structure for Krüppel mRNA was targeted. 2'OMe RNA oligonucleotides were synthesized using standard phosphoramidite chemistry and purified by reverse phase HPLC. 2'OMe RNA probes were synthesized using standard 2'OMe phosphoramidite monomers. Fluorescent dyes were linked to the 5'-end via a Cy5™ Phosphoramidite and Cy3™ Phosphoramidite (Glen Research) respectively [13]. Ion-molecular weights of probes were determined by mass spectrometry using ESI-MASS.

3.2.2. Fluorescence measurements of the hybridization solutions with cyanine dye conjugated RNA probes

Probes and the complementary oligoribonucleotides (ORN) were solved in 10 mM phosphate buffer (100mM NaCl, pH=7.0) (final concentration, 750 nM). Fluorescence emission was measured with a spectrofluorometer (RF-5300PC, Shimadzu). The excitation wavelength of donor fluorophore (pyrene) was 342 nm.

3.2.3. Tm values of probes with the complementary oligoribonucleotides

Melting curves (absorbance versus temperature curves) were measured at 260 nm for the equimolar mixture of the probe and the complementary oligoribonucleotides (ORN) in 10 mM sodium phosphate (pH=7.0) containing 100 mM NaCl. (final concentration, 750 nM).

3.2.4. Visualization of fluorescent dye-conjugated oligoribonucleotides in the presence of ORN

The solutions of hybrids between Cyanine dye-conjugated oligoribonucleotides and the complementary ORN were visualized by UV irradiation at 365 nm using a UV transilluminator (excitation wavelength = 365 nm) with 8 s exposure. Conditions: [OMUpy2] = [ORN] = 3 μM, [Cy3-OMUpy2] = [ORN] = 750 nM, [Cy5-OMUpy2] =

[ORN] = 750 nM in phosphate buffer (10 mM sodium phosphate (pH=7.0) containing 100 mM NaCl).

3.3 Results and Discussion

3.3.1. Probe preparation

Cyanine dye conjugated OMUpy probes used in the presence of study are shown in table. 1. Using our procedures for synthesizing Upy and conventional phosphoramidite methods [13], oligoribonucleotides with cyanine dyes at the 5'-end were synthesized and purified by reversed-phase HPLC.

The obtained oligoribonucleotides were characterized using ESI-MASS. ([Cy3-OMUpy1-5H]$^{-5}$; calcd. 1112.2, found 1112.6, [Cy3-OMUpy2-6H]$^{-6}$; calcd. 960.0, found 960.0, [Cy5-OMUpy1-5H]$^{-5}$; calcd. 1117.4, found 1117.8, [Cy5-OMUpy2-5H]$^{-5}$; calcd. 1447.0, found 1447.1).

Melting curves (absorbance versus temperature curves) were measured at 260 nm for the equimolar mixture of the probe and the complementary oligoribonucleotides (ORN) in 10 mM sodium phosphate (pH=7.0) containing 100 mM NaCl (table.2). The Tm value of OMUnonpy which has no fluorophore modification and ORN was 65 °C. Compared with it, the Tm values of pyrene and cyanine dyes modified probes and ORN were a little lower but they neatly formed duplexes. From these results it is found that Upy, Cy3, and Cy5 hardly affected the stability of the duplex formed by the probe and ORN.

Table 1. Sequences used in the present study.

name	5’ SEQUENCES 3’
Cy3-OMUpy1 (*)	Cy3-*UCC UAA U*Upy*U UGU GCU*
Cy3-OMUpy2	Cy3-*UCC UAA* UpyUpy*U UGU GCU*
Cy5-OMUpy1	Cy5-*UCC UAA U*Upy*U UGU GCU*
Cy5-OMUpy2	Cy5-*UCC UAA* UpyUpy*U UGU GCU*
Cy3-T	Cy3-T
Cy5-T	Cy5-T
OMUpy2	*UCC UAA* UpyUpy*U UGU GCU*
OMUnonpy	*UCC UAA UUU UGU GCU*
ORN	AGC ACA AAA UUA GGA

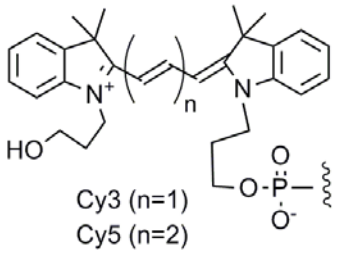

Italic letters: 2’-OMe nucleotides, capital letters: ribonucleotides. Cy5 and Cy3 are conjugated at the 5’ ends of the hydroxyl groups of the nucleotides. (*) The sequence is complementary to the 304-318 nucleotide position of the Kr mRNA (GenBank ID: 22024037).

Table 2. Tm values of probes with the complementary oligonucleotides (ORN).

Probe / ORN	Tm value [℃]
OMUnonpy/ ORN	65
OMUpy1/ ORN	61
OMUpy2/ ORN	60
Cy3-OMUpy1/ ORN	63
Cy3-OMUpy2/ ORN	59
Cy5-OMUpy1/ ORN	62
Cy5-OMUpy2/ ORN	60

Melting temperatures of the equimolar mixture of the probe and ORN in 10 mM sodium phosphate (pH=7.0) containing 100 mM NaCl.

3.3.2. Absorption spectra and fluorescence spectra of Cy3-conjugated oligoribonucleotides and Cy5-conjugated oligoribonucleotides

The fluorescent properties of Cy3-conjugated oligonucleotides were examined (Figure 2a. (2)). Cy3-conjugated oligonucleotides were excited at 342 nm. Cy3-OMUpy2 had faint fluorescence around 480 nm derived from pyrene excimer and strong fluorescence around 570 nm derived from Cy3. The Stokes shift of Cy3-OMUpy2 was nearly 230 nm. Cy3-OMUpy1 also had strong fluorescence around 570 nm with small fluorescence peaking at 378 nm and 398 nm derived from pyrene monomer. In contrast to Cy3-OMUpy1 and Cy3-OMUpy2, Cy3-conjugated thymidine (Cy3-T) had nearly no fluorescence around 570 nm with excitation at 342 nm. These results suggested that Cy3 chromophore conjugated with OMUpy were not directly excited by UV irradiation at 342 nm, but that Upy in Cy3-OMUpy1 and Cy3-OMUpy2 strongly enhanced Cy3 emission. Yamana reported that the pyrene group incorporated into OMUpy1 is intercalated between adjacent nucleobases, and that the fluorescence intensity of OMUpy1 derived from the pyrene monomer around 370 nm is largely quenched due to the formation of exciplexes between pyrene and the nucleobases [14]. In the case of OMUpy2, the fluorescence derived from pyrene monomer was quenched, whereas large fluorescence around 480 nm derived from pyrene excimer was observed in the presence of the complementary RNA [15]. Kawai reported that largely quenched pyrene attached to the DNA strand could serve as a donor for Förster resonance energy transfer (FRET) [16]. Therefore, Cy3 chromophore conjugated to OMUpy2 and OMUpy1 might be excited by FRET from pyrene chromophore under the originally quenched environment.

Next, fluorescence spectra of cyanine dye-conjugated oligoribonucleotides in the presence of the complementary RNA (ORN) were examined. Cy3-OMUpy2/ORN and Cy3-OMUpy1/ORN had strong emission around 570 nm with excitation at 342 nm (Figure 2b. (2)), as in the case of Cy3-conjugated oligoribonucleotides (Figure 2a. (2)). The fluorescence intensity at 570 nm of Cy3-OMUpy2/ORN was four-fold stronger than that of Cy3-OMUpy1/ORN.

We also examined the fluorescent properties of Cy5-conjugated

oligoribonucleotides, (Figure 2c. (2), 2d. (2)). Cy5-OMUpy1 and Cy5-OMUpy2 had strong fluorescence at 670 nm with an extremely large Stokes shift of 330 nm. Compared to Cy3-OMUpy2, Cy5-OMUpy2 has stronger fluorescence around 480 nm. This result suggests that the efficiency of energy transfer might be relatively low. Cy5-OMUpy2/ORN and Cy5-OMUpy1/ORN also had fluorescence around 670 nm with excitation at 342 nm (Figure 2d. (2)). The fluorescence intensity at 670 nm of Cy5-OMUpy2/ORN was a little stronger than that of Cy5-OMUpy1/ORN. It is considered that this result is attributed to the number of pyrene in the OMUpy like a case of Cy3-conjugated oligoribonucleotides.

We showed that cyanine-conjugated OMUpy in the presence of the ORN have strong fluorescence emission derived from cyanine chromophores excited by the emission of pyrene and cyanine-conjugated OMUpy2 are more suitable for the fluorescence detection of the complementary RNA than that of OMUpy1.

(1)

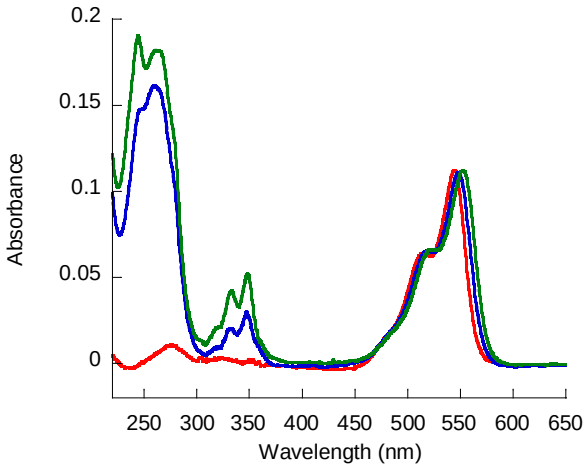

(2)

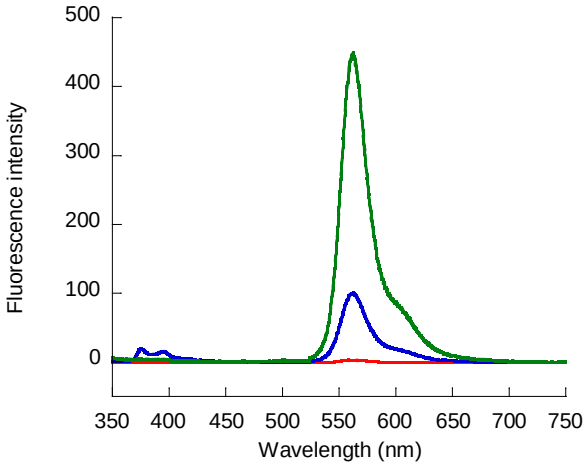

Figure 2a. (1) Absorption spectra and (2) Fluorescence spectra of Cy3-conjugated nucleotides.

[Cy3-OMUpy2] = [Cy3-OMUpy1] = [Cy3-dT] = 750 nM, λex=342 nm, room temperature, green line: Cy3-OMUpy2, blue line: Cy3-OMUpy1, red line: Cy3-dT.

(1)

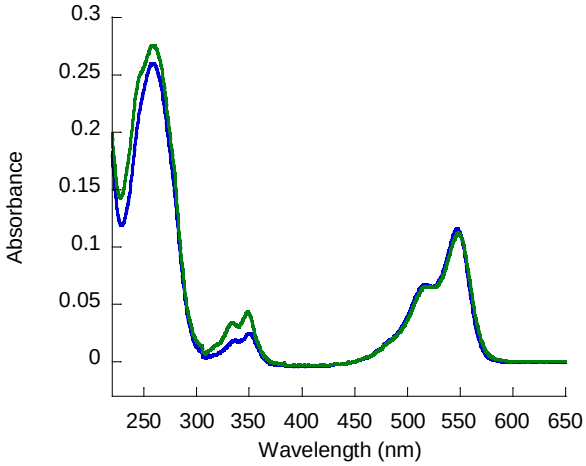

(2)

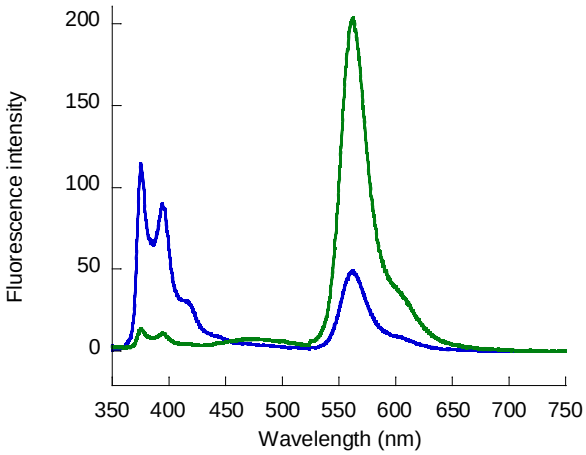

Figure 2b. (1) Absorption spectra and (2) Fluorescence spectra of Cy3-conjugated nucleotides in the presence of ORN.

[Cy3-OMUpy2] = [Cy3-OMUpy1] = [ORN] = 750 nM, λex=342 nm, room temperature, green line: Cy3-OMUpy2/ORN, blue line: Cy3-OMUpy1/ORN.

(1)

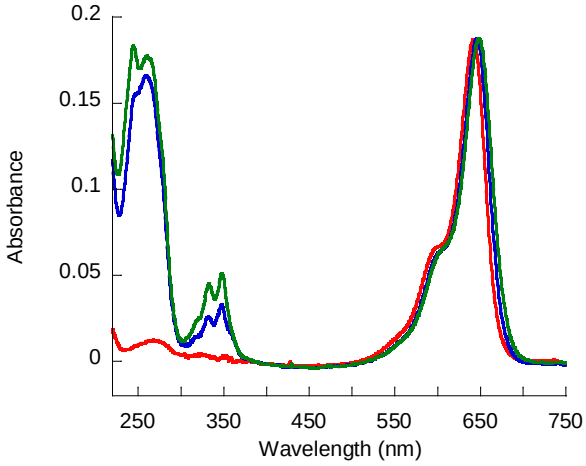

(2)

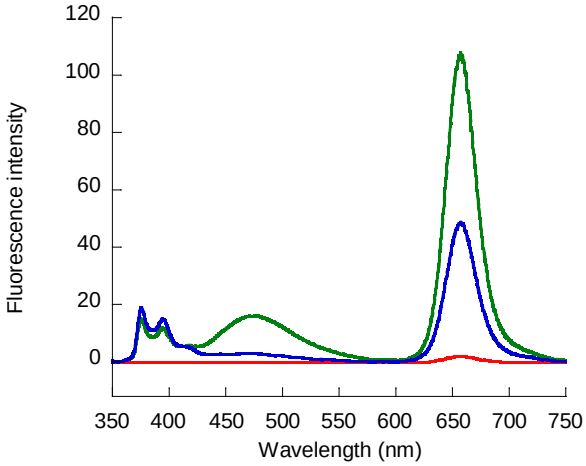

Figure 2c. (1) Absorption spectra and (2) Fluorescence spectra of Cy5-conjugated nucleotides.

[Cy5-OMUpy2] = [Cy5-OMUpy1] = [Cy5-dT] = 750 nM, λex=342 nm, room temperature, green line: Cy5-OMUpy2, blue line: Cy5-OMUpy1, red line: Cy5-dT.

(1)

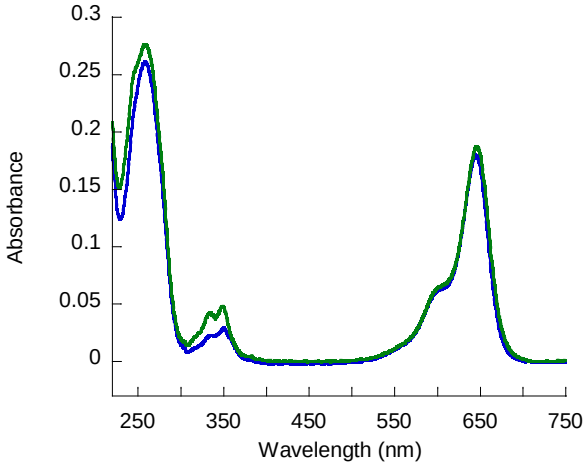

(2)

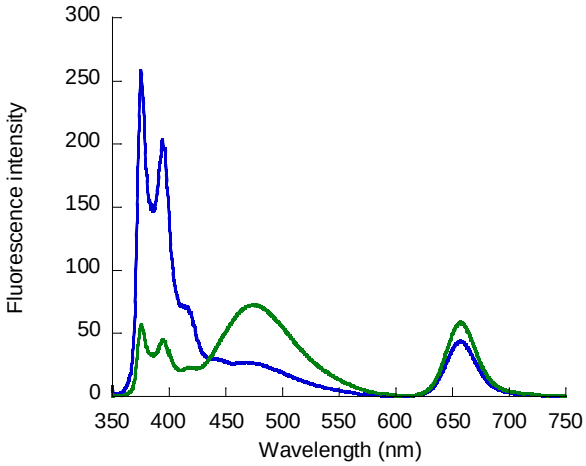

Figure 2d. (1) Absorption spectra and (2) Fluorescence spectra of Cy5-conjugated nucleotides in the presence of ORN.

[Cy5-OMUpy2] = [Cy5-OMUpy1] = [ORN] = 750 nM, λex=342 nm, room temperature, green line: Cy5-OMUpy2/ORN, blue line: Cy5-OMUpy1/ORN.

3.3.3. Visualization of fluorescent dye-conjugated oligoribonucleotides in the presence of ORN

OMUpy2, Cy3-OMUpy2 and Cy5-OMUpy2 in the presence of ORN were visualized by UV irradiation at 365 nm using a UV transilluminator (Figure. 3.). OMUpy2 has blue fluorescence in the presence of ORN. Cy3-OMUpy2 at a concentration of 750 nM emitted bright yellow fluorescent light. Cy5-OMUpy2 gave pink light under the same conditions. These images indicated that Cy3-OMUpy2 and Cy5-OMUpy2 will be feasible to simultaneously visualize multiple RNA targets in a cell by single-excitaion wavelength.

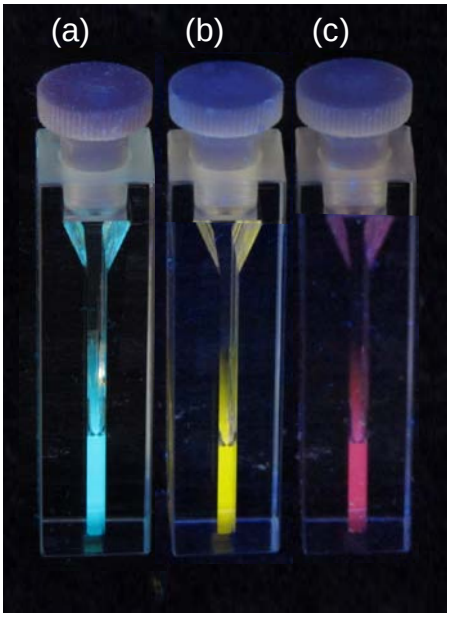

Figure 3. Visualization of fluorescent dye-conjugated oligoribonucleotides in the presesnce of ORN.

(a) [OMUpy2] = [ORN] = 3 μM, (b) [Cy3-OMUpy2] = [ORN] = 750 nM, (c) [Cy5-OMUpy2] = [ORN] = 750 nM in 10 mM sodium phosphate (pH=7.0) containing 100 mM NaCl. The oligoribonucleotides solutions were excited by a UV transilluminator (excitation wavelength = 365 nm) with 8 s exposure.

References

1. Weil, T.T., Parton, R.M., Davis, I. (2010) Making the message clear: visualizing mRNA localization. *Trends Cell Biol*., 20, 380–390.
2. Tekotte, H., Davis, I. (2002) Intracellular mRNA localization: motors move messages. *Trends Genet*., 18, 636-642.
3. Kosman, D., Mizutani, C.M., Lemons, D., Cox, W.G., McGinnis, W., Bier, E. (2004) Multiplex detection of RNA expression in *Drosophila* embryos. *Science*, 305, 846.
4. Levsky, J.M., Shenoy, S.M., Pezo, R.C., Singer, R.H. (2002) Single-cell gene expression profiling. *Science*., 297, 836-840.
5. Macville, M., Veldman, T., Padilla-Nash, H., Wangsa, D., O'Brien, P., Schröck, E., Ried, T. (1997) Spectral karyotyping, a 24-colour FISH technique for the identification of chromosomal rearrangements. *Histochem. Cell Biol*., 108, 299-305.
6. Zimmermann, T., Rietdorf, J., Pepperkok, R. (2003) Spectral imaging and its applications in live cell microscopy. *FEBS Lett.*, *546*, 87-92.
7. Smith, A.M., Nie, S. (2004) Chemical analysis and cellular imaging with quantum dots. *Analyst*, 129, 627-677.
8. Teo, Y.N., Kool, E.T. (2012) DNA-multichromophore systems. *Chem. Rev*., 112, 4221-4245.
9. Teo, Y.N., Kool, E.T. (2009) Polyfluorophore excimers and exciplexes as FRET donors in DNA. *Bioconjugate Chem*., 20, 2371-2380.
10. Tong, A.K., Li, Z., Jones, G.S., Russo, J.J., Ju, J. (2001) Combinatorial fluorescence energy transfer tags for multiplex biological assays. *Nat. Biotechnol*., 19, 756-759.
11. Tong, A.K., Ju, J. (2002) Single nucleotide polymorphism detection by combinatorial fluorescence energy transfer tags and biotinylated dideoxynucleotides. *Nucleic Acids Res.*, 30, e19.
12. Ohya,Y., Yabuki, K., Hashimoto, M., Nakajima, A., Ouchi, T. (2003) Multistep fluorescence resonance energy transfer in sequential chromophore array constructed on oligo-DNA assemblies. *Bioconjugate Chem.*, 14, 1057-1066.
13. Wincott, F., DiRenzo, A., Shaffer, C., Grimm, S., Tracz, D., Workman, C., Sweedler, D., Gonzalez, C., Scaringe, S., Usman, N. (1995) Synthesis, deprotection, analysis and purification of RNA and ribozymes. *Nucleic Acids Res.*, 23, 14, 2677-2684.
14. Nakamura, M., Fukunaga, Y., Sasa, K., Ohtoshi, Y., Kanaori, K., Hayashi, H., Nakano, H., Yamana, K. (2005) Pyrene is highly emissive when attached to the RNA duplex but not to the DNA duplex: the structural basis of this difference. *Nucleic Acids Res*., 18, 5887-5895.
15. Mahara, A., Iwase, R., Sakamoto, T., Yamana, K., Yamaoka, T., Murakami, A. (2002) Bispyrene-conjugated 2'-*O*-methyloligonucleotide as a highly specific

RNA-recognition probe. *Angew. Chem. Int. Ed.*, 41, 3648-3650.

16. Kawai, K., Kawabata, K., Tojo, S., Majima, T. (2002) Synthesis of ODNs containing 4-methylamino-1, 8-naphthalimide as a fluorescence probe in DNA. *Bioorg. Med. Chem.*, 12, 2363-2366.

Summary

Chapter 1.

The detection of mRNA expressed in *Drosophila* embryo using OMUpy2 was described. The performance of OMUpy2 for RNA detection was estimated using oligo RNA solution, total RNA extracted from *Drosophila* embryo, and *Drosophila* embryo. In this thesis, OMUpy2 was used as RNA-specific probe. OMUpy2 emitted fluorescence at 480 nm only when it hybridized with its complementary RNA in homogeneous media. OMUpy2 also emitted similar fluorescence around 480 nm in total RNA extracted from *Drosophila* embryos containing a large amount of RNA other than target mRNA. These results suggest that target mRNA in total RNA extracts was successfully detected by OMUpy2. Furthermore, from the fluorescence intensity of OMUpy2, relative mRNA expression levels could be estimated. The detection of target mRNA in *Drosophila* fixed embryo was carried out using Kr-OMUpy2, and the emission was observed in the center region of the fixed embryo. It was confirmed that the emission observed in the embryo treated with Kr-OMUpy2 was derived from bis-pyrene by the fluorescence spectrum measured with a microspectroscope under the microscope.

Chapter 2.

The average molecule numbers of target RNA expressed in a HeLa cell were estimated using OMUpy2. In general, inferring the exact RNA expression level is difficult, but even approximation of RNA expression level would give us useful information to assist the diagnosis and the judgment of progress, and prognosis for various diseases. We examined whether the abundance of target RNA in total RNA extracted from HeLa cells could be estimated using OMUpy2. Two characteristics of OMUpy2 make it possible to estimate the expression level of target RNA in total RNA extract. The first is that OMUpy2 binds to target RNA in a one-to-one. Second is that OMUpy2 emits fluorescence at around 480 nm only when it bound to target RNA. In order to create the calibration plots of the fluorescence intensity at 480 nm

corresponding to cORN concentration, the fluorescence intensity at 480 nm of OMUpy2 in the presence of cORN was measured in the range of 10 nM to 1000 nM cORN concentration. The expression levels of 28S rRNA, mir-21, mir-24, mir-29, and U6 snRNA in a HeLa cell were calculated from the calibration plots of the fluorescence intensity at 480 nm corresponding to ORN concentration, respectively.

Chapter 3.

The development of multi-colored RNA FRET probes to simultaneously observe multiple target RNAs was described. The excitation and fluorescence wavelength of Cy3 are 550 nm and 570 nm, respectively. Those of Cy5 are 650 nm and 670 nm, respectively. Both Cy3 and Cy5 emitted no fluorescence with 342 nm excitation. However OMUpy2 modified with Cy3, Cy3-OMUpy2, emitted fluorescence at around 650 nm with 342 nm excitation. OMUpy2 modified with Cy5, Cy5-OMUpy2, emitted fluorescence at around 670 nm with 342 nm excitation. FRET might be occurred from pyrene in OMUpy2 to Cy3 or Cy5. Equimolar mixtures of OMUpy2 and oligo RNA, Cy3-OMUpy2 and oligo RNA, and Cy5-OMUpy2 and oligo RNA solutions emitted blue, yellow, and pink fluorescence, respectively, by the excitation at 342 nm. These results suggest that these probes are applicable to simultaneous detection of multiple target RNAs in a cell.

List of Publications

Chapter 1: Ueda, T., Kobori, A., Yamayoshi, A., Yoshida, H., Yamaguchi, M., Murakami, A.
RNA-based diagnosis in a multicellular specimen by whole mount in situ hybridization using an RNA-specific probe
Bioorganic & Medicinal Chemistry, 20, 6034-6039. (2012)
doi: 10.1016/j.bmc.2012.08.028.

Chapter 2: Ueda, T., Murakami, A.
Quantitative analysis of RNA expression with RNA specific probes
In preparation

Chapter 3: Kobori, A., Ueda, T., Sanada, Y., Yamayoshi, A., Murakami, A.
Dual-Fluorescent RNA Probes with an Extremely Large Stokes Shift
Biosci. Biotechnol. Biochem., 77, 1117-1119. (2013)
doi:10.1271/bbb.121018

Acknowledgements

The present study in this doctoral dissertation was carried out under the guidance of Professor Akira Murakami at the Bio-regulation Science Laboratory of the Department of Molecular Engineering, Kyoto Institute of Technology from 2006 to 2013.

It would not have been possible to write this doctoral dissertation without the help and support of the kind people around me. I would like to express my sincere gratitude to them here.

I am grateful to Professor Akira Murakami for giving me the opportunity to study under his group and his guidance. I am also grateful to Professor Masamitsu Yamaguchi for his collaboration, advice on writing papers, and direction of microinjection technique. I would like to thank Associate professor Akio Kobori for his suggestion and advice on writing papers. I appreciate Assistant professor Asako Yamayoshi and Hideki Yoshida for their discussion and advices.

I also thank my friends and members of the Bio-regulation Science laboratory and Chromosome technology laboratory for their help and support.

Last but not the least, I would like to extend my deepest gratitude to my family, Makoto Ueda, Makiko Ueda, Tomoko Ueda, and Hiroko Ueda. Without their encouragement, support, and patience over a long period of time, my doctoral dissertation could not have been accomplished. I’ m really grateful for all the family.

April 4, 2013

TAKAKO UEDA